Deutsches Zentrum
DLR für Luft- und Raumfahrt

Work Package WP15

Methodology for testing, assessment and characterization

of storage technologies and materials

Task 4

New Measurement Systems for PCM Storage

Deliverable Report 15.4

Feasibility of the new PCM measurement system based on the "electric resistance approach" in lab scale demonstrated

Solar Facilities for the European Research Area (SFERA) Project

Date: June 2012

PREPARED BY:

Thomas Bauer, Doerte Laing, Wolf-Dieter Steinmann

German Aerospace Center (DLR), Germany

CONTRIBUTORS:

Roman Adinberg, David Zvegilsky, Leon Peters

Weizmann Institute of Science, Israel

Contents

Abstract

In the frame of Task 4/WP-15, a lab-scale setup based upon the “electric resistance approach” has been developed and put into operation to measure the charging/discharging status of a phase change material (PCM) storage system.

PCM storage systems are favourable for direct steam generation (DSG) plants. At the moment, temperature sensors detect the charging/discharging status of these systems. However, during charging/discharging the system has a temperature plateau and is isothermal. For this reason, the charging status, defined as the ratio of the mass fraction of liquid PCM to the total PCM mass, cannot be detected directly. As a consequence, WP 15 Task 4 aims to identify alternative parameters and methods to determine the charging status of PCM storage systems.

For high-temperature PCM systems, other sensor systems than temperature sensors have not been previously considered. Hence, this report outlines an overview and classification of alternative methods. Existing alternative PCM measurement methods in the low temperature range are reviewed (e.g., ice storage). The adaptation of these methods to the high temperature range is assessed. Intrinsic properties, such as optical transparency, electric resistance and density, of high-temperature PCM (anhydrous salts) are evaluated.

The selected alternative measurement approach detects differences between the solid and liquid phase of the PCM in terms of the electrical resistivity and the filling level due to density changes. One major challenge of this approach is the electrode design in the high-temperature environment. Lab-scale tests with several different electrodes were performed. Within the project a novel electrode was developed (patent pending). The design allows for the integration of the electrode in a PCM storage system. For the electric resistance approach suitable measurement parameters (e.g., frequency, voltage) were identified. Within the project, a signal generation and data acquisition unit was developed. Also, a graphical user interface within the control software of the PCM-storage was programmed. A lab-scale experimental setup clearly demonstrated differences in the electrical conductivity of several orders of a magnitude between the solid and the liquid phases of high-temperature PCMs. The feasibility of the detection of the charging/discharging status on larger-scale systems was proved. Measurements with electrodes on a prototype storage system with about 160 kg PCM demonstrated the approach.

Keywords: Phase change materials (PCM), latent heat storage, high-temperature electrode

Nomenclature:

CSP – concentrating solar power

DSG – direct steam generation

HTF – heat transfer fluid

$NaNO_3$ – Sodium nitrate

KNO_3 – Potassium nitrate

PCM – phase change material

1. Introduction

Concentrating solar power (CSP) plants differ among each other in terms of the heat transfer fluids (HTFs). HTFs include thermal oil, molten salt, air and water/steam. PCM storage systems are a suitable option for the two-phase heat transfer fluid water/steam in DSG plants [1]. Phase change materials (PCM) considered in the literature for latent heat storage cover a wide temperature range from -100 °C to 1000 °C (Figure 1). DSG plants require PCMs with a phase change temperature in the range 200 to 350 °C. Typical PCMs are inorganic alkali nitrate/nitrite salts and their mixtures. One example is sodium nitrate ($NaNO_3$) with a melting temperature of 306 °C and a melting enthalpy of 178 J/g. Another example is an eutectic mixture of 54wt% potassium nitrate (KNO_3) and 46wt% $NaNO_3$ with a melting temperature of 222 °C and a melting enthalpy of 108 J/g.

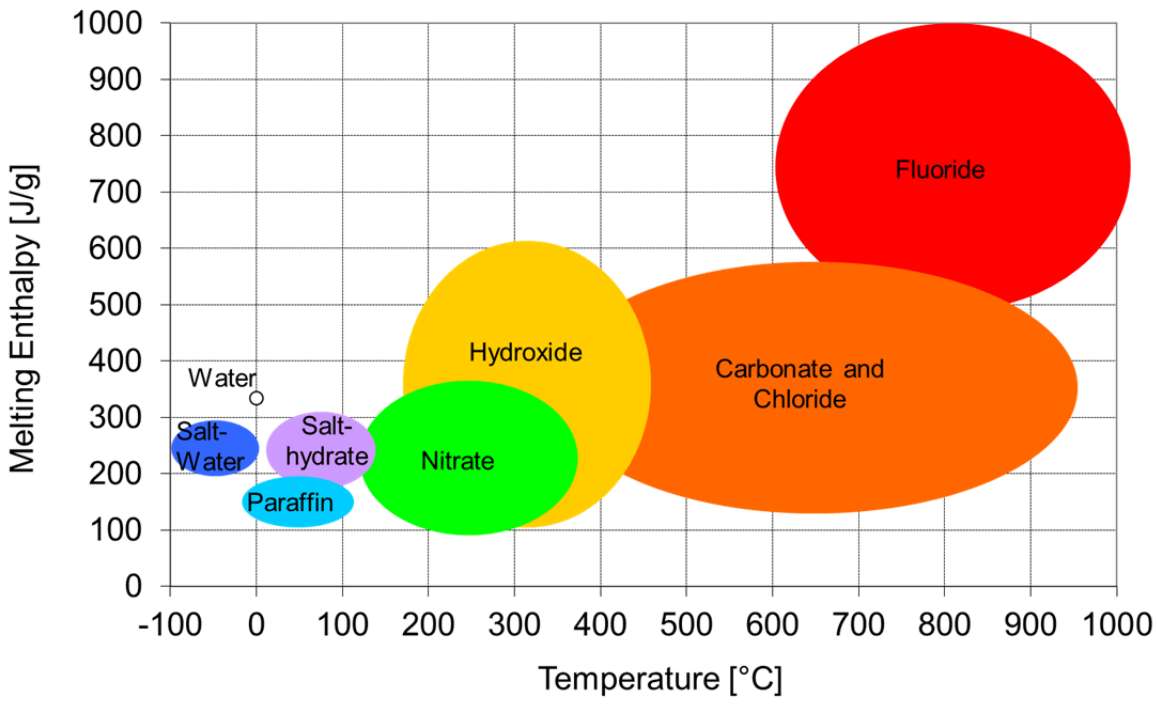

Figure 1. Overview of PCM classes as a function of temperature.

For high-temperature PCM storage system developments, current systems utilize temperature sensors to gain information on the charging/discharging status of these systems. The charging status can be defined as the ratio of the mass fraction of liquid PCM to the

total PCM mass. Figure 2 shows the detected temperature signal during charging (plateau with dashed red ellipse on the left hand side) and during discharging (plateau with dashed red ellipse on the right hand side). For PCM storage, these isothermal plateaus are characteristic. However, the detected temperatures cannot be easily correlated to the charging status of the PCM storage. In particular this is true for PCM-storage operation with partial charging/discharging and operation close to the phase change temperature. As a consequence, the work reported here aims to identify alternative parameters and methods to determine the charging status of the PCM storage.

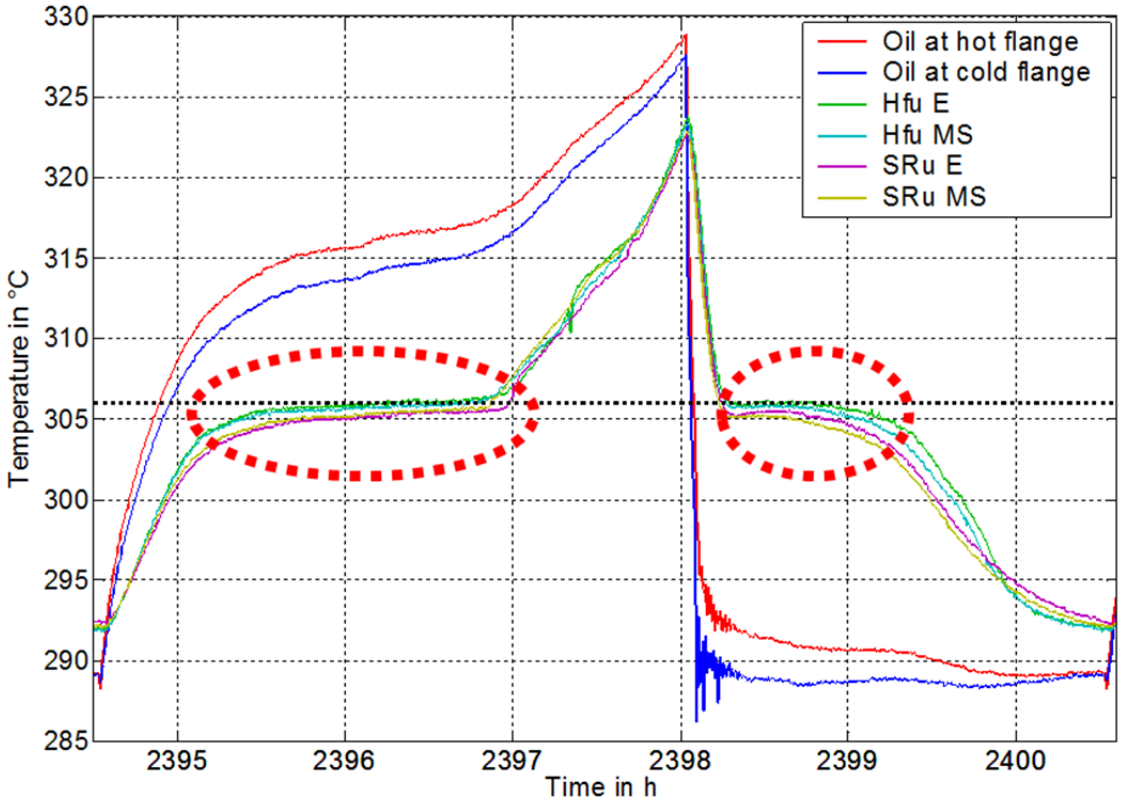

Figure 2. Signals of temperature sensors in a PCM storage unit with $NaNO_3$ during the charging and discharging process.

The charge and discharge power of PCM-storage systems is typically limited by the poor thermal conductivity of PCM. It has been demonstrated that the finned tube design can effectively overcome this limitation. Figure 3 shows schematically the growth of the PCM on the fins during the solidification (discharge) process. The figure schematically shows that complex solidification fronts will form within PCM storage systems with fins. Additionally, voids form in the solidification process due to PCM contraction.

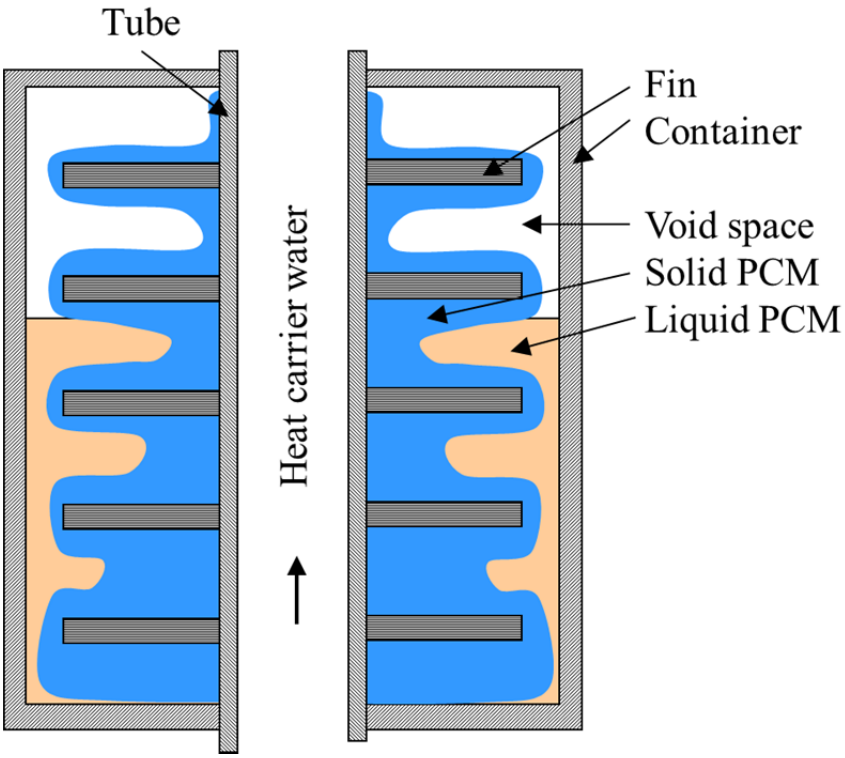

Figure 3. Scheme of a PCM-storage with water/steam as heat carrier in a tube and fins within the storage material volume; the scheme shows the status during discharging.

Section 2 is a critical literature review on relevant research and development on PCM-storage measurement methods, high-temperature electrode designs and intrinsic material properties of high-temperature PCMs. Section 3 focuses on lab-scale and large-scale experiments on high-temperature PCM measurement methods.

2. Theoretical part

2.1. PCM measurement methods for ice storage systems

There are at least two methods for measuring the charging status of water/ice PCM storage systems. The thickness of growing ice layer on the heat exchanger surface can be detected by the difference in electrical conductivity between ice (solid PCM) and water (liquid PCM). Figure 4 on the right hand side shows a sensor design with a series of electrodes. Another method measures the water level in the PCM tank (Figure 4 left). The measurement is based on the difference of conductivity between air (gas phase) and water (liquid PCM).

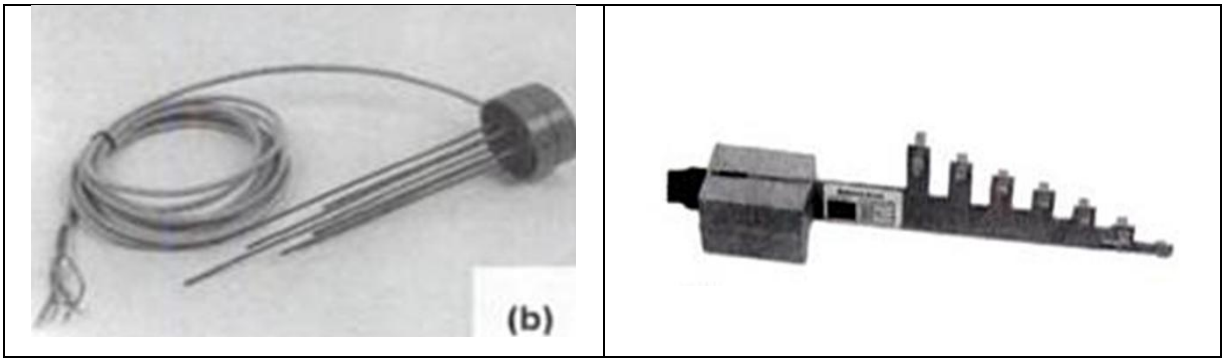

Figure 4. Commercial ice-storage sensors: water level sensor (left) and electrical conductivity ice-layer sensor (right) [2].

It should be noted that there is a significant difference between water/ice and most of the other PCMs. Water increases about 9 % in volume when it changes to ice. In other words, the volume change on melting related to the solid phase $\Delta V/V_s$ of water/ice is negative, whereas almost all PCMs have a positive value. This aspect has a direct impact on the design of the sensor system. Hence, it is not possible to directly transfer ice storage concepts to other PCMs with a positive $\Delta V/V_s$ value.

Ezan et al. developed a measurement method to determine the solidification front in an ice storage system [3]. They classified the electrical conductivity measurement methods, which can be used for monitoring ice formation, as follows:

- Resistance measurement using Ohm's law and alternating and direct current circuits
- Inductance based measurement methods
- Capacitance based measurement methods, which utilizes the dielectric effect

2.2. PCM measurement methods for paraffin Storage systems

Researchers examined alternative PCM measurement methods for paraffin PCM-storage systems at the Brandenburg University of Technology within a research project [4]. The following intrinsic PCM properties of paraffin were analysed:

- Dielectric constant
- Ultrasonic velocity and ultrasonic attenuation
- Thermal expansion of encapsulated paraffin
- Optical transparency

For further development, the optical transparency was selected. An optical sensor was engineered for the paraffin PCM storage. In addition, for PCM-composites in walls, a heat flux sensor was engineered and tested.

2.3. High-temperature electrode design

Several applications require suitable high-temperature electrodes. As "high-temperature", electrode operation beyond 300 °C is considered. At temperatures beyond 300 °C, polymers such as PE, PTFE and PEEK are thermally not stable. Hence, electrical insulator made of polymers cannot be used. High temperature, high pressure and corrosive media applications typically utilize ceramic electrical insulator. Hence, these high-temperature electrodes require a suitable metal-ceramic joint design. The following are selected examples of areas for high-temperature electrodes with ceramic-metal joints:

- Electrodes for molten metals [5]
- Electrodes for water/steam multiple-phase flow [6]
- Ignition electrode for internal combustion engines
- (Reference) electrodes for corrosion at high-temperatures [7]

These high-temperature electrodes with ceramic-metal joints are based on a rigid (inflexible) design. Figure 5 shows rigid high-temperature electrodes for molten metals as an example. Non-rigid high-temperature electrode designs could not be identified.

Figure 5. Photograph of rigid electrodes for molten metals [5].

2.4. Intrinsic material properties of high-temperature PCMs

In order to identify a suitable measurement approach, some relevant material properties of anhydrous alkali metal nitrate salts are reviewed.

For molten salts, the physical properties can be divided into non-electrolyte and electrolyte properties. Molten salts have non-electrolyte properties similar in magnitude to those of room temperature liquids, in spite of the obvious temperature differences [8]. The molten alkali nitrate salts are clear waterlike liquids. Potentially glass fibre sensors could be installed in the PCM to detect the transparency. Own experiments on alkali metal nitrate salts showed that the **transparency** depends on different aspects. For example, different cooling rates result in different crystal sizes and transparencies (e.g. for $NaNO_3$). Some $Ca(NO_3)_2$ rich melts also form glass phases which are highly transparent in the solid phase. Opaque white samples have also been obtained (e.g. KNO_3-$NaNO_3$ eutectic). Due to the heterogeneous behaviour, sensor development on transparency detection was discontinued.

Bloom states that the **dielectric constant** of molten salt electrolytes is not known but many investigators arbitrarily assign it to a value of 3 or 4 [8]. Frederikse gives dielectric constants of different anhydrous solid salts. The dielectric constant depends on temperature, frequency and direction (for anisotropic solids). Typical values of alkali nitrate salts range from 4 to 10 in the solid phase [9]. The capacity is directly proportional to the dielectric constant for several simple geometries (e.g., parallel plate arrangement, concentric cylinders) [10]. Within this work, capacity measurements on the difference between molten and solid salt were performed. However, the temperature effect was strong compared to differences between solid and liquid phase. Hence, this method was not developed further.

The gas phase has a low dielectric constant with values close to unity. Work on capacitive filling level sensors to distinguish between molten salt and gas phase was not carried out.

Figure 6 shows the **density** of sodium nitrate in the liquid and solid phase. It can be seen that the density decreases in the solid and liquid phase with increasing temperature. At the melting temperature of 306 °C, there is a large volume change of melting ΔV compared to the volume of the solid salt at the melting temperature V_s. The value $\Delta V/V_s$ is about 11 %. In other words, a filling level of a fully charged molten PCM storage of 100 % can be assumed. In the solidification process the salt significantly contracts and some voids are formed.

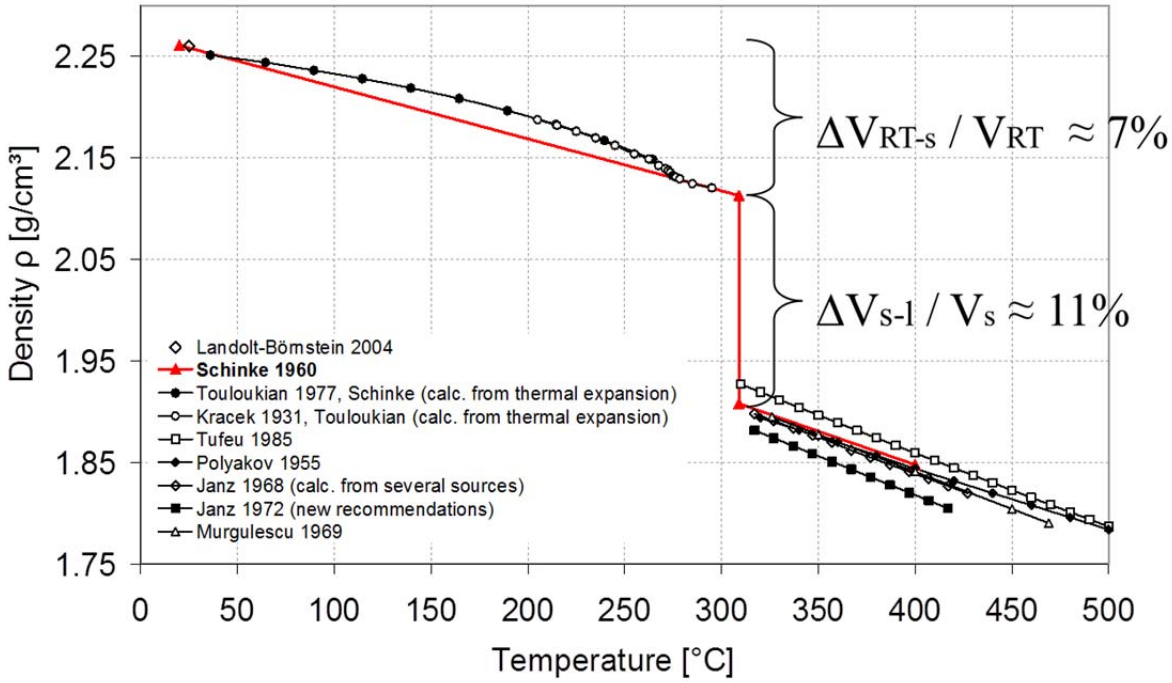

Figure 6. Density of sodium nitrate ($NaNO_3$) as a function of temperature [11].

Figure 7 plots the **electrical conductivity** of two alkali metal nitrates and one salt mixture. It can be seen that all salts have similar electrical conductivities in the liquid phase. The electrical conductivity is almost constant in the liquid phase. In the solid phase, the electrical conductivity steadily increases from room temperature to below the melting temperature. Upon melting the electrical conductivity increases about two orders of magnitude.

Figure 7 also compares the electrical conductivity to other materials. At room temperature, alkali metal nitrate salts are insulators. Just below the melting temperature, they are semiconductors with a low electrical conductivity. Above the melting temperature, they are semiconductors with a high electrical conductivity.

For the further development, electrical and spatial (density) based methods were selected. For these intrinsic material properties, differences between the solid and liquid alkali nitrate PCM can be clearly detected.

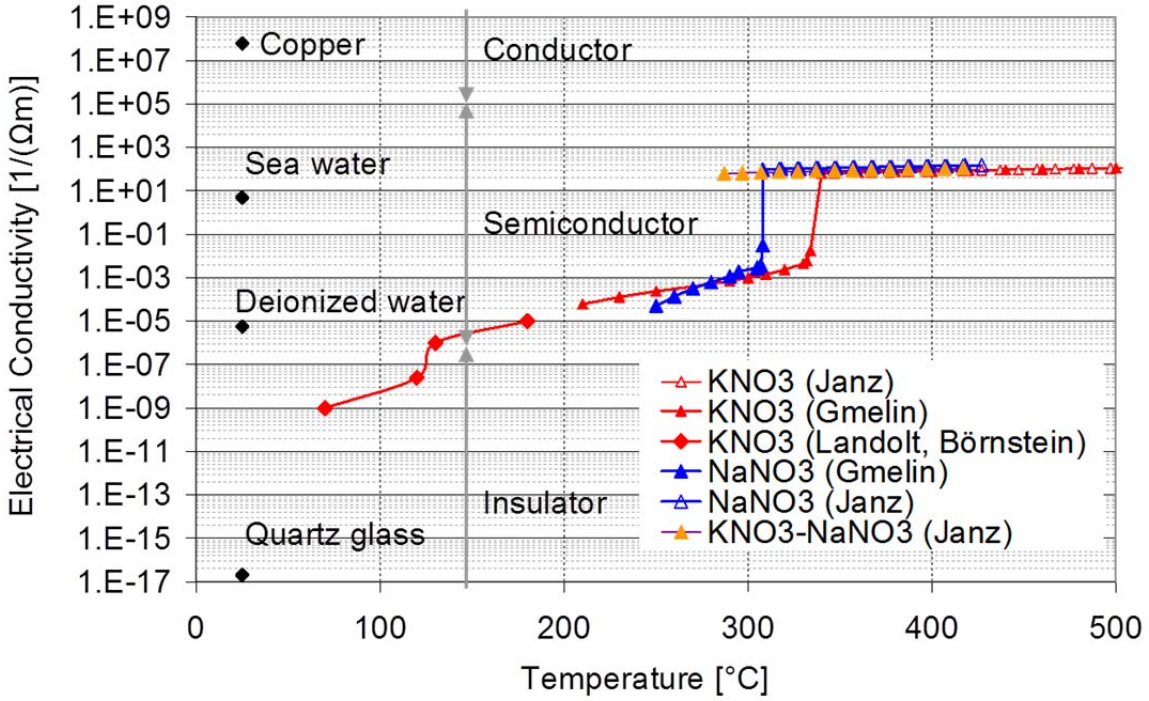

Figure 7. Electrical conductivity of alkali metal nitrates vs. temperature [12-14].

2.5. Summary

The major findings of the literature review can be summarized as follows:

- There are lessons to be learned from commercial ice-storage systems for high-temperature PCM storage measurement devices.
- There are not only two phase in a PCM storage system (usually solid and liquid), but also a third gas phase due to the volume expansion on melting (or PCM contraction during solidification).
- Additional fins in the storage volume lead to more complex distributions of solid PCM, liquid PCM and voids compared to designs without fins.
- Flexible high-temperature electrodes (similar to flexible mineral insulated thermocouples) to detect different PCM phases and voids could not be identified.
- The management of partial-load operation of PCM storage system is critical. For ice storage systems, this aspect is described. In order to ensure reliable operation, additional ice thickness sensors are utilized.
- The methods can be classified in two broad categories. These are external concepts based on the heat balance of the PCM systems (1) and internal concepts (2). Internal concepts utilize intrinsic PCM property changes during the process of melting and solidification (e.g. electrical, optical and spatial). Figure 8 summarizes the major measurement methods described in literature.

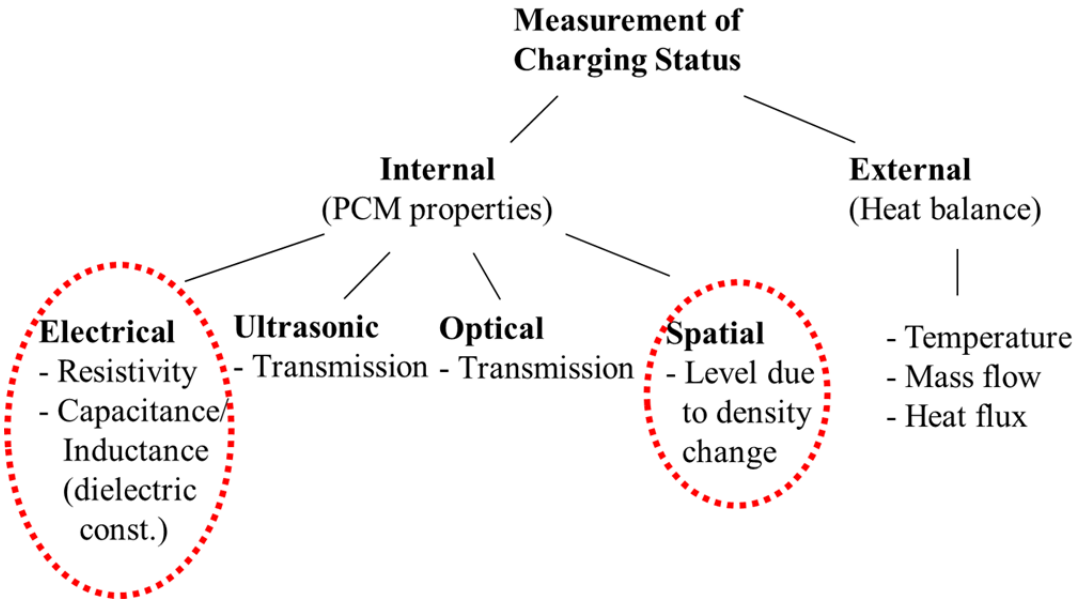

Figure 8. Classification of PCM measuring methods.

3. Experimental part

3.1. Lab-scale experiments

Molten salts are usually good ionic conductors with high electrical conductance values [Bloom]. Electrical conductivity measurements with direct current result in undesirable ion movement in the melt. Hence, measurements with alternating sine current were performed.

For lab-scale experiments a eutectic mixture of 54wt% potassium nitrate (KNO_3) and 46wt% sodium nitrate ($NaNO_3$) was prepared. The crucible material was aluminium oxide. The two electrodes were made of aluminium foil. The temperature of the solid and molten salt was monitored by a mineral insulated type K thermocouple within the salt. The setup was placed on top of a heating plate (Figure 9).

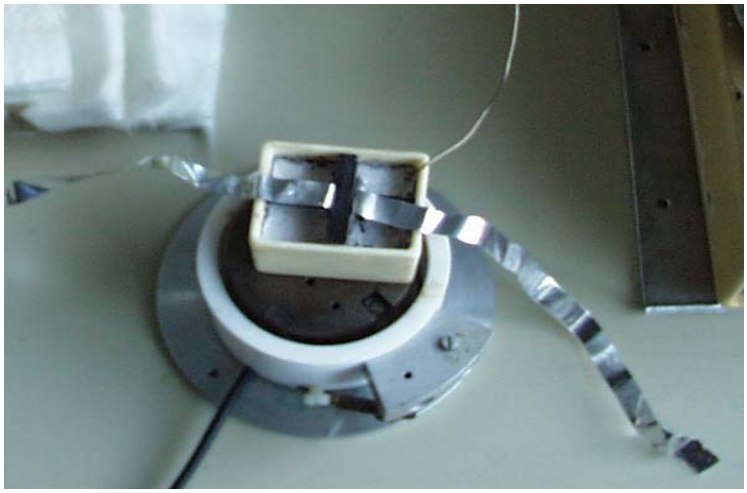

Figure 9. Photograph of the Setup with KNO_3-$NaNO_3$ salt, aluminium stripes as electrodes, aluminium oxide crucible and heating plate without insulation (left)

In total, three different circuit setups were realized (Figure 10). For the first impedance measurements (Setup 1), a commercial precision LCR-meter (Agilent 5284A Precision) was utilized. Subsequently, a second setup with commonly available measurement equipment was analysed (oscilloscope, frequency generator, measuring resistor). The second setup led to a third setup which is discussed in the next section (prototype development).

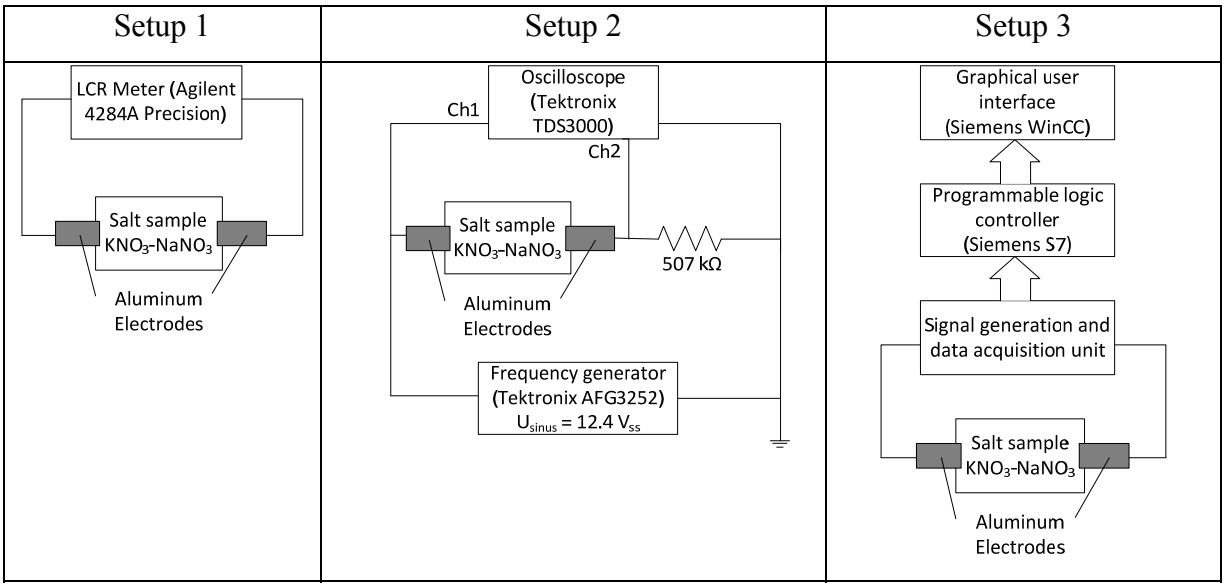

Figure 10. Circuit diagrams of three measurement setups: RLC-meter (Setup 1), resistor measurements (Setup 2) and final data acquisition for large-scale experiments (Setup 3).

Figure 11 plots experimental results of Setup 1 and Setup 2 using different frequencies. It can be seen that results of the two measurement setups agree closely for the three frequencies 107 Hz, 1 kHz and 10 kHz. Measurements show high impedance values in the solid phase of the salt (below the melting temperature of 222 °C). The drop of the impedance from the solid phase to the liquid phase could be clearly detected (for both methods and for all frequencies). Impedance values were higher for lower frequencies for most cases. Measurements in the solid phase just below the melting temperature were an exception with similar values for all frequencies. Overall, the measurements demonstrated the feasibility of the "electric resistance approach" in a lab-scale experiment.

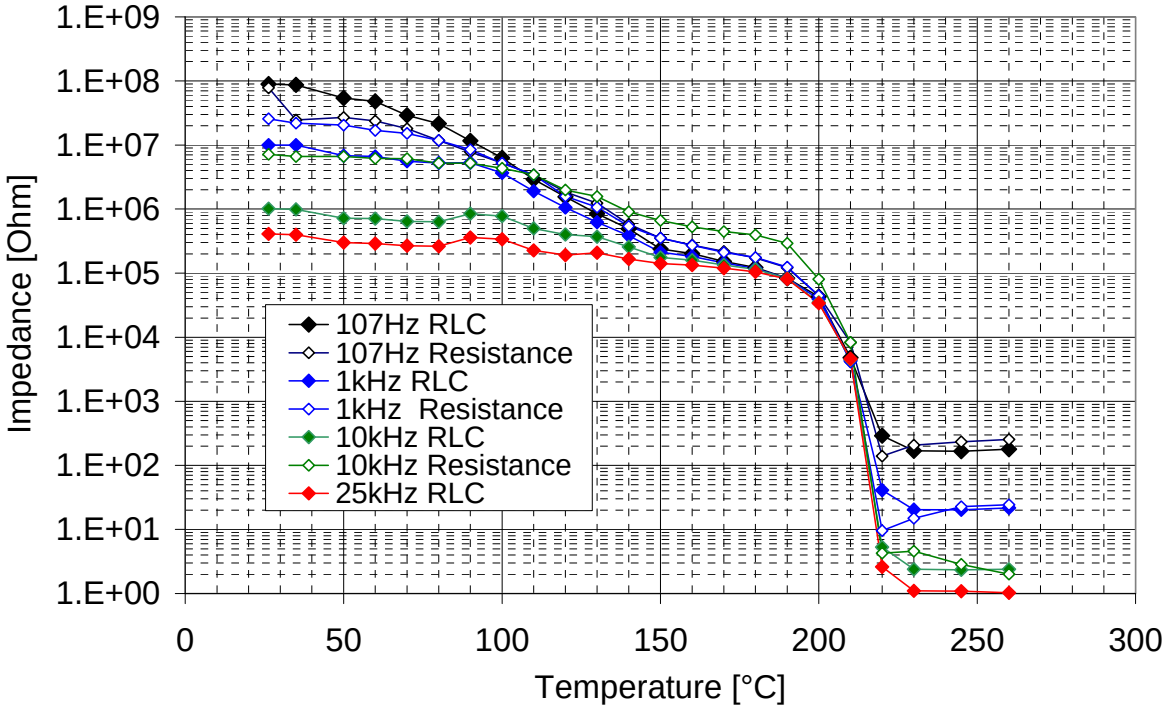

Figure 11. Results of impedance measurements of KNO_3-$NaNO_3$ with Setup 1 and Setup 2.

3.2. High-temperature electrode development

In order to detect the charging/discharging status of PCM-systems, designs with multiple electrodes are required. Figure 12 shows a design with 0.3 mm stainless steel wires in horizontal and vertical direction as electrodes and a high-temperature resistant polyimide frame (Sintimid PUR HT, Ensinger GmbH). The design aimed to detect the PCM melting front at each cross-point of the horizontal and vertical wires.

Results show that the detection of the phase front may only be feasible for the melting process. Also, it would be necessary to locate the feed wires within the solidified PCM. Hence, the design shown in Figure 12 would result in some major limitations for the detection of the charging/discharging status of PCM-systems. It was concluded that a design with electrically isolated electrodes is advantageous.

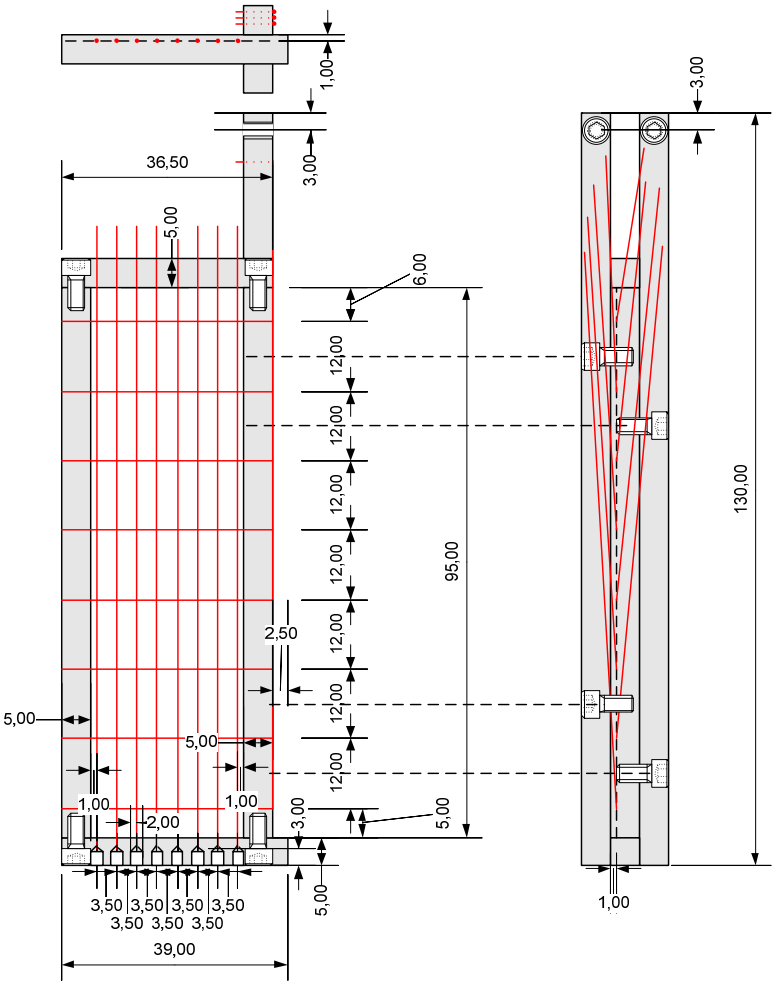

Figure 12. First high-temperature electrode design with stainless steel wire (in red) as electrodes and high-temperature resistant polyimide frame (grey).

Figure 13 shows lab-scale tests on an assembly with multiple electrical insulated electrodes in order to detect the melting front in PCM-storage systems. As an electrical insulator, a high-temperature resistant hollow polyimide assembly was utilized. Eight M3 stainless steel screws within this assembly served as electrodes. Compressed expanded graphite (CEG) plates next to the assembly increased the heat transfer and led to a uniform melting front. Figure 14 shows similar lab-scale tests using multiple glass capillary tubes which include a stainless steel wire.

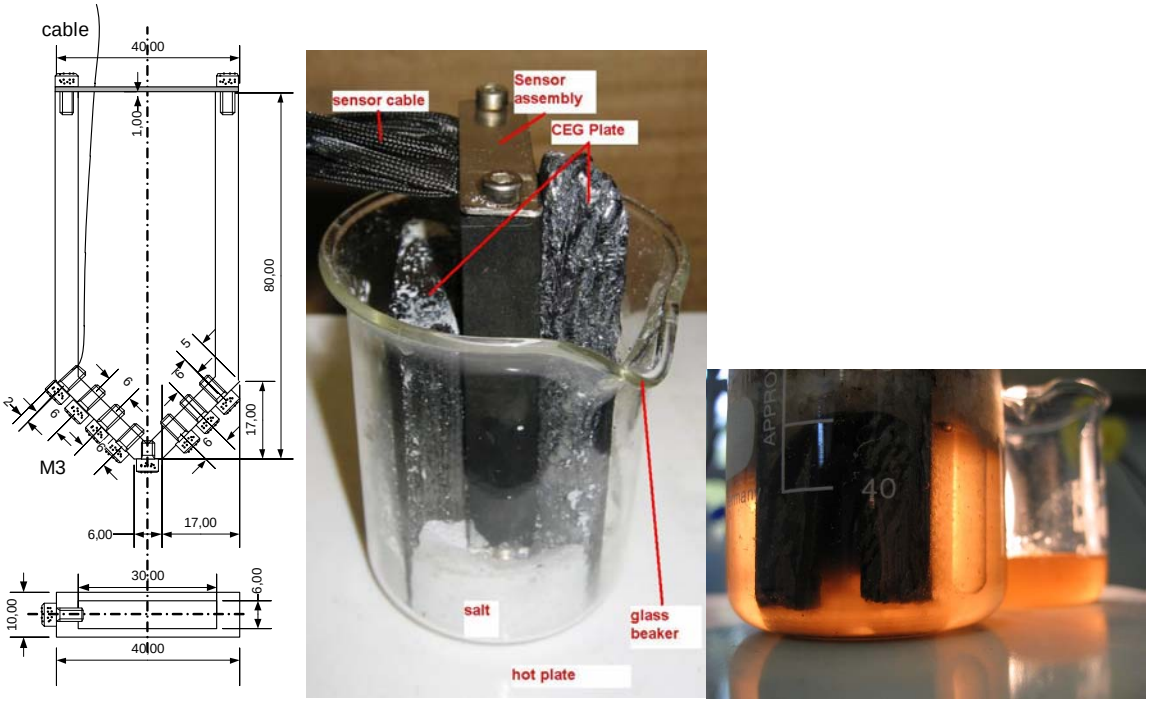

Figure 13. High-temperature electrode design with stainless steel screws as electrodes and high-temperature resistant polyimide assembly as electrical insulator; technical drawing (left), photograph of the setup with solidified salt (middle) and photograph of part of the setup with partial molten salt at the bottom (right).

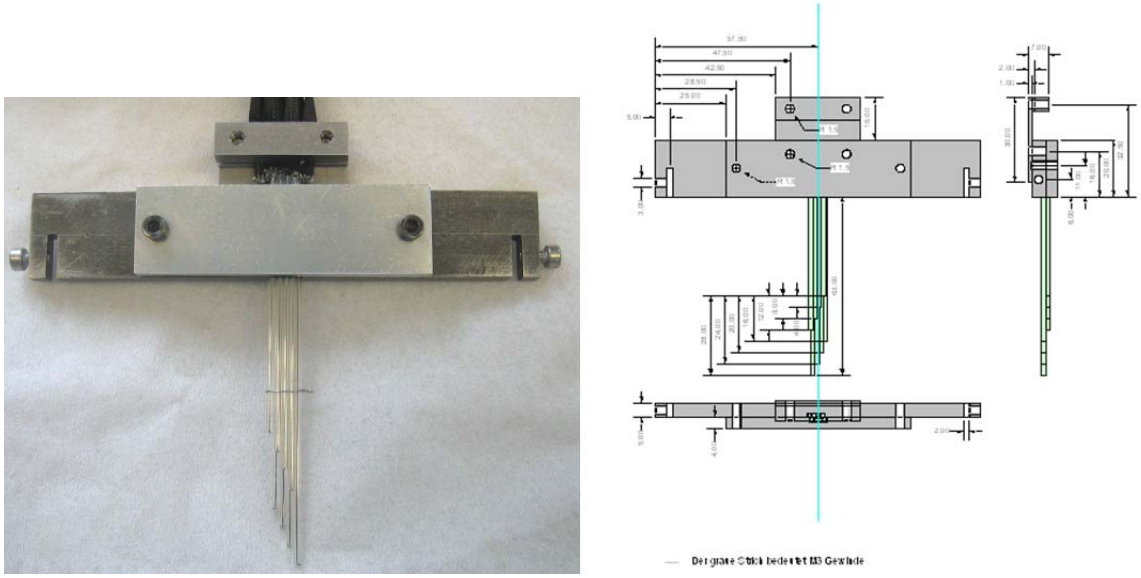

Figure 14. High-temperature electrode design with stainless steel wire as electrodes within glass capillary tubes as electrical insulator.

Experiments with the three setups (Figure 12 to 14) showed that the PCM melting front can be detected. For example, Figure 15 shows the measurement signals vs. time of the melting of a solidified PCM block on a hot plate of the setup shown in Figure 14. However,

some major limitations occurred. They included the leak tightness of the screw-polyimide joint, the fragility of the glass capillary tubes, creeping molten salt within glass capillary tubes and a maximum temperature limit of about 300 ° due to the polyimide. Also, no suitable design for larger assemblies in a PCM-storage could be identified.

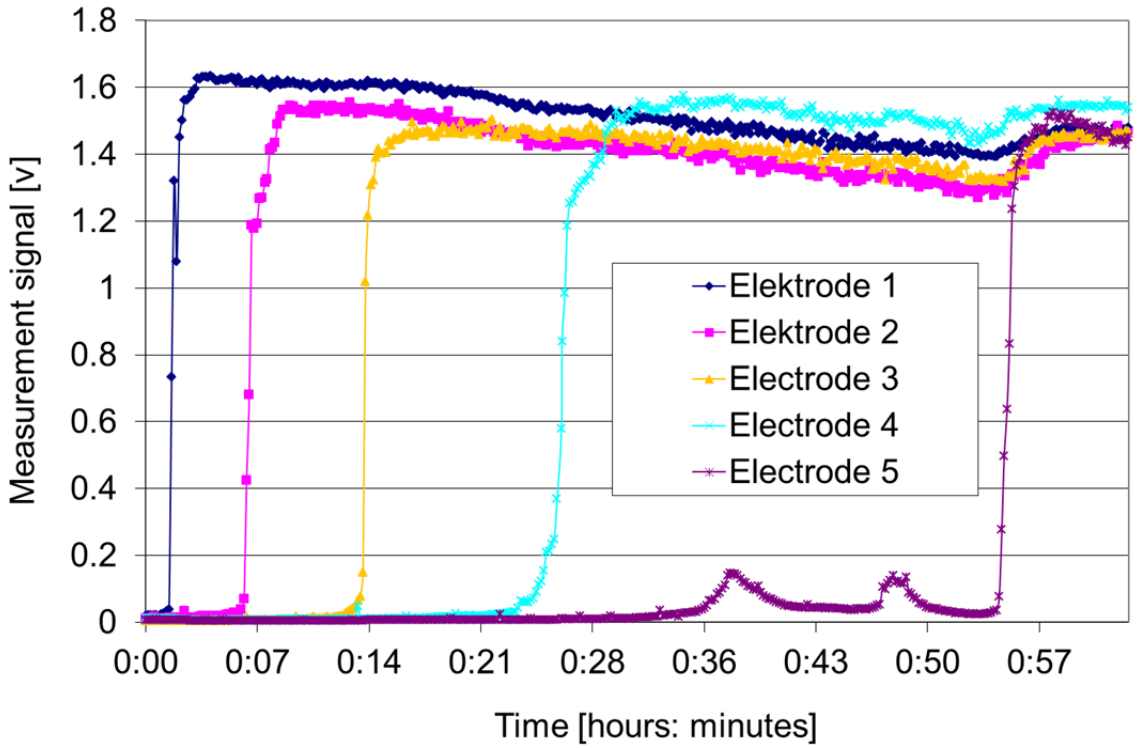

Figure 15. Measurement results of the high-temperature electrode design with stainless steel wire as electrodes within glass capillary tubes as electrical insulator.

Another high-temperature electrode design utilized two wire (or stripe) spirals on a rod. Figure 15 shows different setups that were tested. As electrode materials aluminium foil stripes and stain steel wires with 0.3 mm diameter were used. Rods were made of polyimide and glass. The rods were immersed in a glass beaker filled with alkali metal nitrate salt. The melting front progressed from the bottom to the top of the beaker using a hot plate (similar to the setup shown in Figure 13 on the right hand side). Previous assemblies (Figure 12 to 14) focused on single point measurements. The setup shown in Figure 16 focused on a continuous detection of the melting front of the PCM in one dimension along the rod. The amount of liquid PCM was correlated to the electrical resistance between the two spirals. In order to increase the sensitivity of the method, spirals rather than two straight rods were used.

Measurement results for the melting process of a solidified PCM from the bottom to the top showed that the measured resistance could be clearly correlated to the height of the

melting front along the rod (or amount of liquid PCM compared to the total PCM mass). Based on the equivalent circuit diagram of the two wire electrode (Figure 16 right), it can be shown that there is a non-linear correlation between the melting front position and the total impedance (Figure 17). Figure 17 plots measurement results of the aluminium foil electrode and confirms the theoretical prediction from the equivalent circuit diagram. Overall, it seems feasible to detect for example a molten salt filling level with this setup. Limitations of this continuous detection method include the following: fragile glass rods, temperature limitation of the polyimide, limitation to melting processes in only one direction or filling levels measurements.

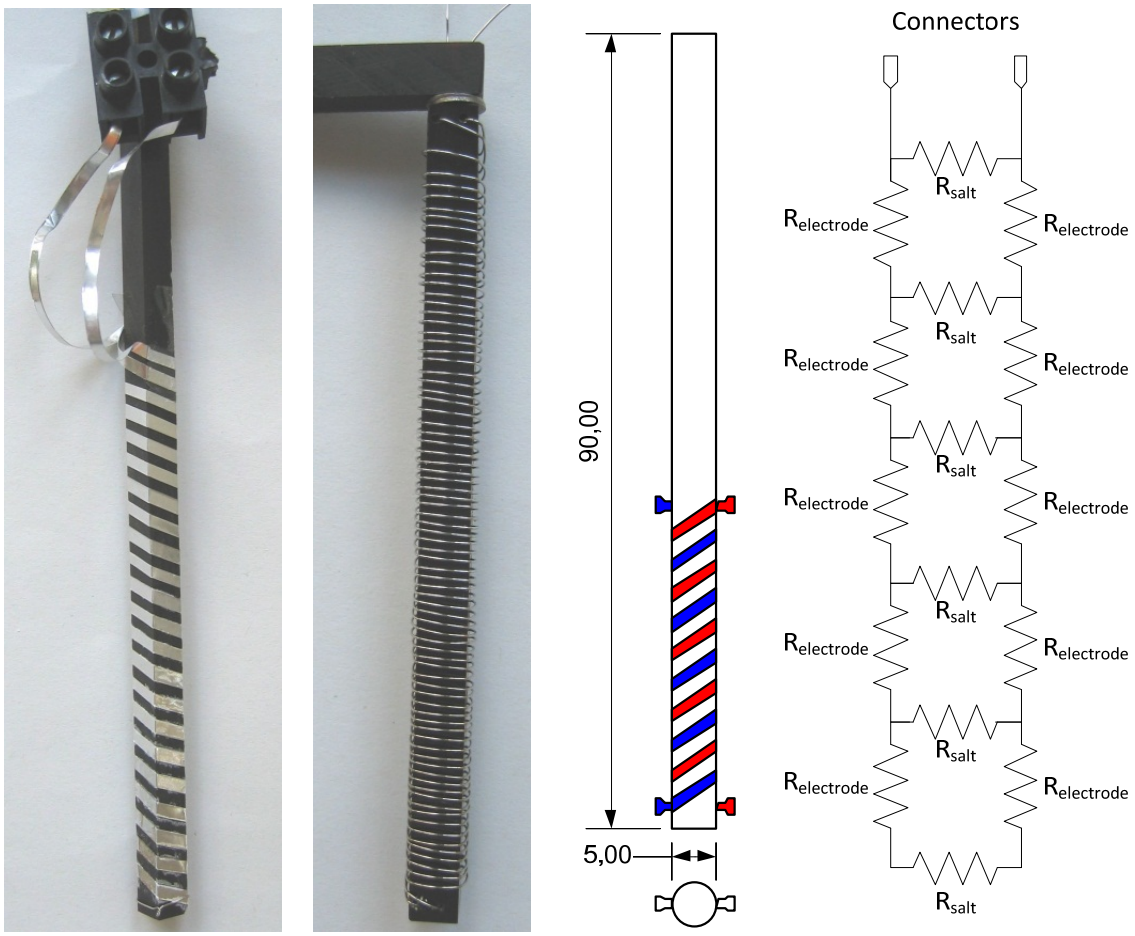

Figure 16. High-temperature electrode design with two wire spirals as electrodes on a rod; polyimide rod with aluminium foil (left), polyimide rod with stainless steel wire (middle left) glass rod with stainless steel wire (middle right) and equivalent circuit diagram (right).

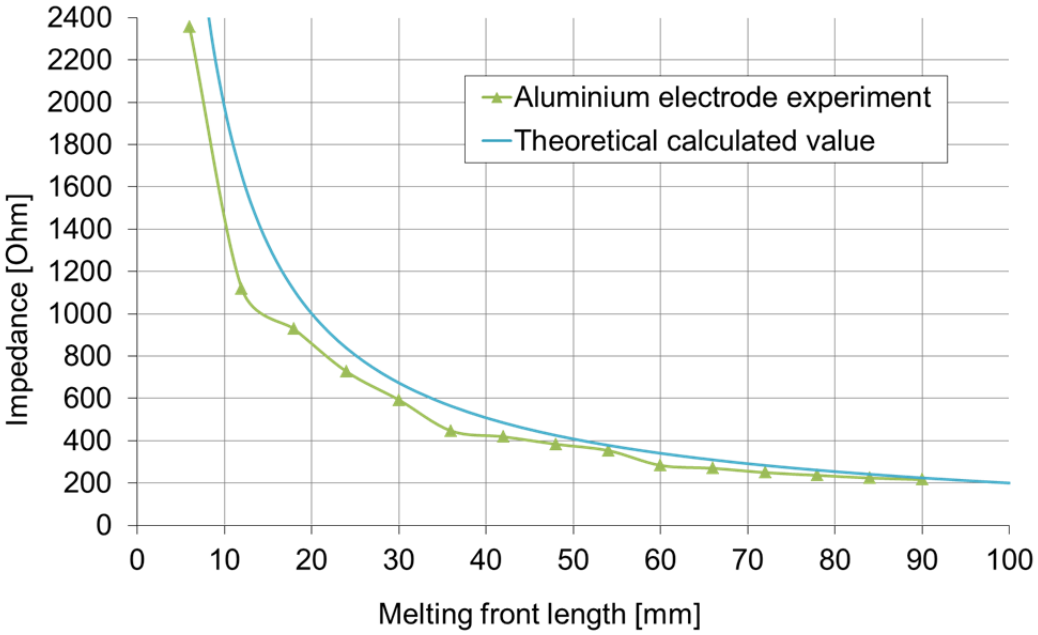

Figure 17. Measurement result and theoretical predicted values of aluminium foil electrode for the continuous detection of the melting front.

The described initial experiments (Figure 12 to 16) led to the following electrode requirements: high-temperature resistant (> 300 °C), electrically insulated measurement tip, flexible integration in the PCM-storage unit (e.g., like mineral insulated thermocouples), detection of the two PCM phases **and** voids/gas phase.

In order to meet these requirements, an alternative electrode design was developed. Based on commercially available components, a first prototype electrode was constructed by laser welding within the project (Figure 18). The electrode design includes a metallic measurement tip, a ceramic-metal-joint, a ceramic isolator and a metallic tube filled with electrically insolating powder (published patent [15]).

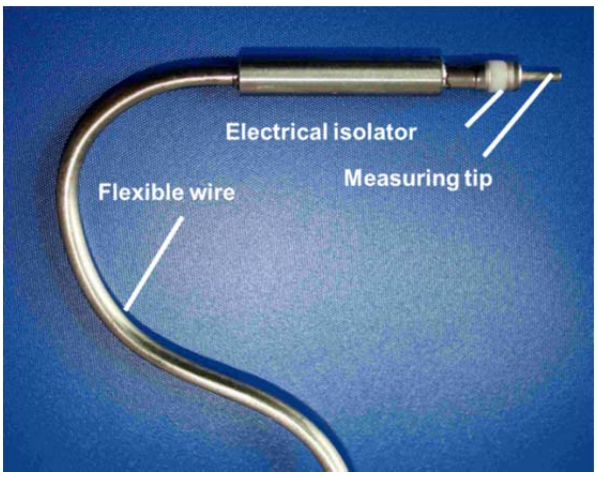

Figure 18. Photograph of novel high-temperature electrode.

Based on the first two measurement setups (Figure 10), a third setup was designed. The customized electronic circuit included sinus signal generation, signal processing, multiplexing of electrodes and data acquisition. Figure 19 shows a photograph of the signal generation and data acquisition unit. This unit was integrated in an existing programmable logic controller (Siemens SPS). Figure 20 shows the wiring diagram of the electronic measurement devices. This third setup not only included hardware development, but also software developments. Software developments included microcontroller programming of the signal generation and data acquisition unit and the programmable logic controller with graphical user interface (Siemens Step7 and WinCC). Figure 21 shows a screenshot of the graphical user interface to display electrode signals.

Figure 19. Photo of the signal generation and data acquisition unit with microcontroller.

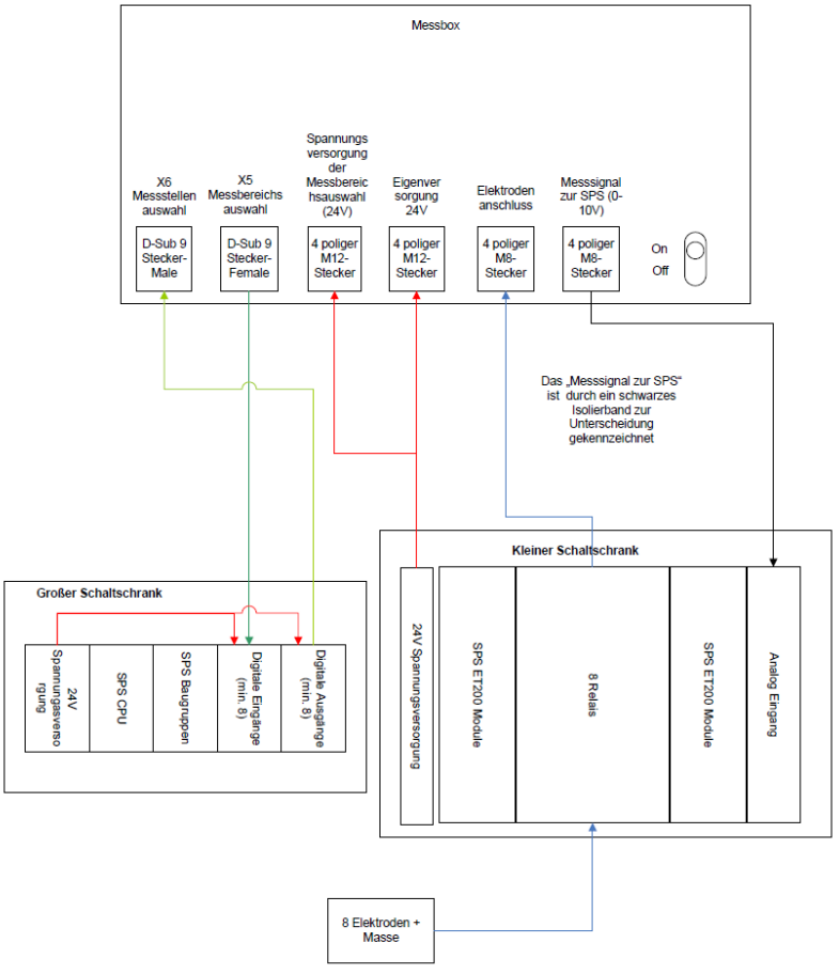

Figure 20. Interconnection of the signal generation and data acquisition unit and the programmable logic controller (SPS).

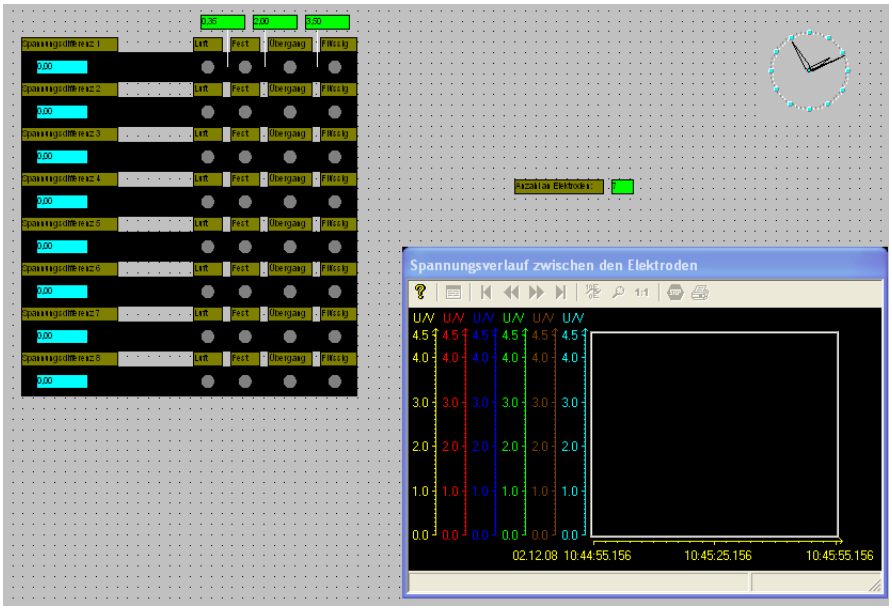

Figure 21. Graphical user interface to display electrode signals.

A feasibility test of PCM-measurement electrodes on an existing PCM prototype storage system was carried out. Figure 22 gives schemes and photographs of this prototype system. The prototype consists of a tube register with aluminium fins (Figure 22, middle right) and a container filled with PCM (Figure 22, left). The heat transfer fluid within the tubes was thermal oil. There is a void space between this finned register and the PCM container. This void space contained six stainless steel rods (diameter about 2 mm) with different lengths (Figure 22, right).

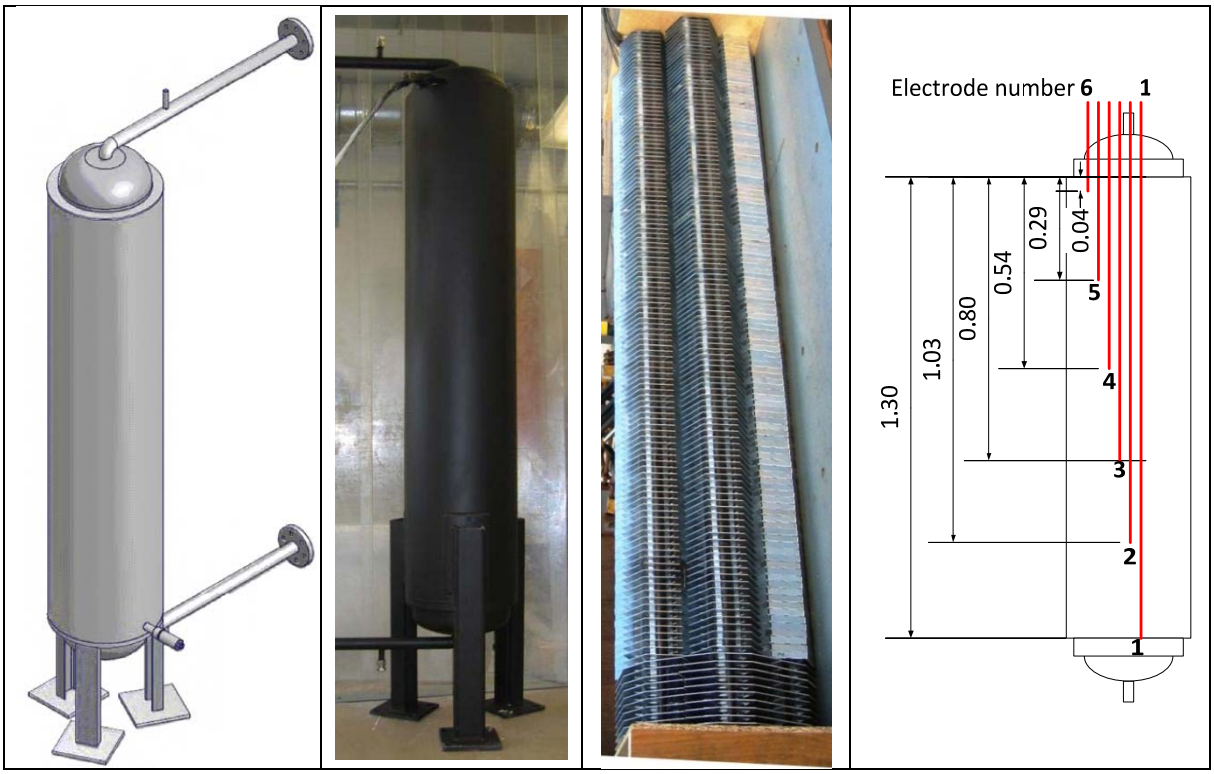

Figure 22. Integration of electrodes in a PCM-prototype storage system; scheme of the storage system without insulation (left), photograph of the storage system (middle left), photograph of the integrated tube register with aluminium fins (middle right) and position of the electrodes within the PCM volume (right).

For the charging and discharging processes, the thermal oil inlet temperature of the PCM-storage system is kept constant by an external heating and cooling thermal oil loop. As a PCM sodium nitrate with a melting temperature of 306 °C was utilized. First, the storage system was fully charged. The thermal oil inlet temperature and the fully liquefied PCM had a temperature of about 330 °C. The PCM has a low density (or high volume) in the liquid phase. Hence, all electrodes are covered by molten salt. This results in a low

voltage (or low resistance) as shown in Figure 23 at the time zero (value about 0.2 V for all electrodes).

The discharging process, or the solidification of the PCM, was initiated by lowering the thermal oil inlet temperature to 290 °C. Figure 23 shows that after a short period of time a constant thermal oil inlet is reached. The PCM contracts upon solidification. This leads to a lower molten salt filling level within the electrode space next to the container walls. Measurement results show that Electrode 6 (top electrode) has reached the maximum detectable resistance value after about 30 Minutes. This can be attributed to the sinking molten salt level in the PCM container and air surrounding Electrode 6. After some time, Electrode 5 and 4 also detect a rising electrical resistance. Unlike Electrode 6, all other electrodes did not detect the maximum resistance values. This aspect could be caused by frozen salt rather than air surrounding the Electrodes 1 to 5. The Electrodes 1 to 3 detected almost the same signals. This indicates a similar solidification process of the salt region in the lower part of the storage system. After about 5 hours, a constant thermal oil outlet temperature was reached. After this time period, also electrode signals were almost constant. Hence, the solidification process within the PCM-storage system could be clearly detected by the "electric resistance approach".

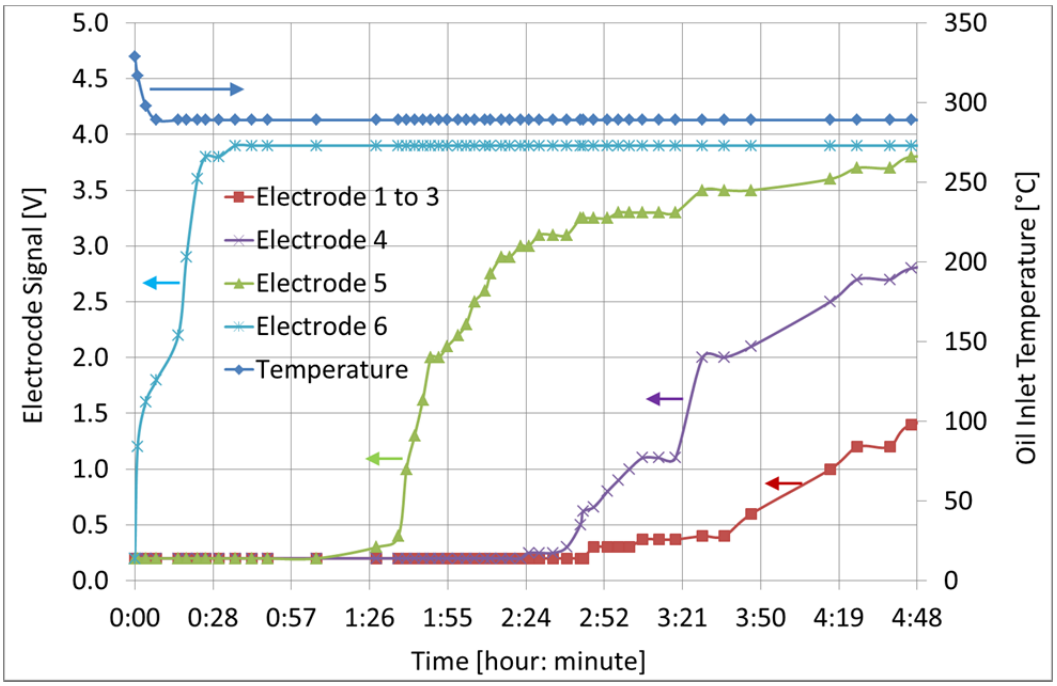

Figure 23. Measurement results of the "electric resistance approach" on an existing PCM storage system.

4. Summary and conclusion

At the time of writing, there is no convincing method readily available to determine accurately the charging/discharging status of high-temperature phase change material (PCM) storage systems for solar direct steam generation plants. The limitation of simple temperature sensors in PCM systems was outlined. Partial load operation of PCM storage is an example of temperature sensor limitations. Such operation modes clearly require novel alternative concepts to measure the charging/discharging status of PCM storage systems. The reported work reviewed developments for low-temperature PCM storage systems. In particular commercial ice storage systems utilize successfully alternative measurement methods. Hence, there are lessons to be learned from ice storage systems. However, knowledge of ice-storage system cannot be simply transferred to high-temperature PCM systems. There are oppositional characteristics on the volume change on melting. Also, high-temperature electrode design is inherently more difficult due to the limited material choice.

For alternative measurement methods, intrinsic material properties of high-temperature PCMs were evaluated. They included the transparency, dielectric constant, density and electrical conductivity of alkali metal nitrates. It was found that transparency and dielectric constant properties are less suitable. There are pronounced differences in solid and liquid values of the density and the electrical conductivity of alkali metal nitrate salts. Hence, the further development focused on changes in these properties. Density changes can result in spatial level changes of molten salt in the PCM storage. Alkali metal nitrates are poor electrical conductors in the solid phase and they are good ionic conductors in the liquid phase.

In lab-scale test the electrical conductivity in the solid and liquid phase of alkali metal nitrate salts was analysed. Suitable measurement parameters, such as voltage and frequency levels were identified. For the selected “electric resistance approach”, no suitable high-temperature electrode could be identified. In this work several different electrode designs were developed. Tests of these designs revealed the major limitations such as leak tightness of components for low viscosity molten salts, fragility of the glass and ceramic electrodes, up-scaling and integration of electrodes in storage systems and limitations with regard to the material choice of the high-temperature resistant electric isolator. In order to

overcome most of the limitations, within the project a novel electrode was developed (patent pending).

Another major focus was the integration of the alternative PCM measurement method with several electrodes in an existing prototype latent heat storage system. A customized electronic circuit included sinus signal generation, signal processing, multiplexing of electrodes and data acquisition was designed. This design not only included hardware, but also some major software developments. We tested the alternative PCM measurement method using several electrodes in a PCM-prototype storage system with thermal oil as a heat transfer fluid and sodium nitrate with a melting temperature of 306 °C as a PCM. Measurements with the signal generation and data acquisition unit and the PCM-prototype storage system clearly demonstrated the feasibility to detect the charging/discharging status with the alternative PCM measurement method.

5. Acknowledgement

We express our thanks especially to Robert Lindemann, Uli Schollenbruch, Andreas Weniger, Andreas Haagen and Raymond A. Pitty Cabrera for the experimental part and data analysis in this work. The author wish to thank the European Union for the financial support given to the Solar Facilities for the European Research Area (SFERA) project (Grant Agreement No. 228296).

6. References

[1] Laing, D., C. Bahl, et al. (2011). Combined storage system developments for direct steam generation in solar thermal power plants. ISES Solar World Congress 28.8. – 2.9.2011, Kassel, Germany.

[2] Dincer, I., Rosen, M.A. (2002). Thermal Energy Storage - Systems and Applications. New York, Chichester, John Wiley & Sons.

[3] Ezan, M. A., L. Cetin, et al. (2011). "Ice thickness measurement method for thermal energy storage unit." Journal of Thermal Science and Technology 31(1): 1-10.

[4] Fischer, U. R., U. Maschke, et al. (2009). Entwicklung eines Messverfahrens zur Bestimmung des thermischen Beladungsgrades von PCM-Paraffin-Speichern. Bundesministeriums für Wirtschaft und Technologie (BMWi), BMWi-Projekt 0327370F.

[5] Sensors for Molten Metals (2012) Heraeus Electro-Nite, Online: http://electro-nite.de/en/sensorsformoltenmetals/sensors_molten_metals.aspx (accessed 18.6.2012)

[6] Schleicher, E. (2012) Conductivity and Temperature Needle Probes, Helmholtz-Zentrum Dresden-Rossendorf (HZDR), Germany, in collaboration with FZZ Feinmechanisches Fertigungszentrum, Germany, Online: http://www.hzdr.de/db/Cms?pOid=11942&pNid=1690 (accessed 18.6.2012)

[7] High Temperature Reference Electrode (2012) MPM Technologies, Inc., US, Online: http://www.mpmtechnologies.com/High-Temp-Reference-Electrode.htm (accessed 18.6.2012)

[8] Bloom, H. (1967). The Chemistry of Molten Salts, Benjamin, Inc.

[9] Frederikse, H.P.R. (2008) Permittivity (Dielectric Constant) of Inorganic Solids, CRC. Handbook of Chemistry and Physics, CRC Press.

[10] Lindner, H., H. Brauer, et al. (1998). Taschenbuch der Elektrotechnik und Elektronik, Fachbuchverlag Leipzig.

[11] Bauer, T., D. Laing, et al. (2012). "Characterization of Sodium Nitrate as Phase Change Material." International Journal of Thermophysics 33(1): 91-104.

[12] Janz, G.J., Allen, C.B., Bansal, N.P., Murphy, R.M., Tomkins, R.P.T. (1979) Physical Properties Data Compilations Relevant to Energy Storage. II. Molten Salts: Data on Single and Multi-Component Systems, NSRDS-NBS 61 Part II (National Standard Reference Data Series)

[13] Landolt, Börnstein (2004) KNO3, in Numerical data and functional relationships in science and technology, Group III: Condensed Matter, Volume 36, Subvolume B1.

[14] Gmelin (1938) Gmelins Handbuch der anorganischen Chemie, Natriumnitrat und Kaliumnitrat, Deutsche Chemische Gesellschaft, Verlag Chemie GmbH, S. 270-297, 269-323.

[15] Bauer, T., Steinmann, W.-D. (2011) Electrode design for latent heat storage, German Patent DE102010001361A1.

Project SFERA

Solar Facilities for the European Research Area

Milestone 15.5

Feasibility of the new PCM measurement system for calorimetric and heat flow parameters in lab scale demonstrated

Report

Roman Adinberg, David Zvegilsky, Leon Peters

Solar Research Facilities Unit

The Weizmann Institute of Science

Rehovot 76100, Israel

September 2011

Contents

Abstract

In the frame of Task 4/WP-15, a lab set-up based upon the RHTS (reflux heat transfer storage) concept has been developed and put into operation to measure the calorimetric and heat transfer properties of phase changing materials utilized for thermal storage in a temperature range between 200 and 400^{o}C.

Initially, this system was designed for testing the compatibility and thermal stability of storage materials used in the RHTS system developed as part of the EU-funded FW6 DISTOR project (contract no. SES6-CT-2004-503526). It was shown that the lab system has highly efficient heat transfer characteristics proper to thermosyphons and pool boilers and the capability to operate as a calorimeter aimed to quantify the variable latent heat storage capacity during thermal charge and discharge cycles.

Presently, this capability has been expanded for different phase change materials such as metal alloys and molten inorganic salts having a melting/eutectic point within the prescribed temperature range relevant to the solar parabolic trough CSP (concentrating solar power) systems. In addition, this work involved investigating errors inherent in measurements taken by the system, mitigating thermal losses to the environment, and calibrating the mass flow rate of the heat transfer fluid (HTF, e.g. Dowtherm-A) circulating through a closed loop of pipes in the system by natural convection under varied process conditions.

This report outlines in detail the PCM (phase change material) measurement system design and describes a mathematical model developed for thermal analysis and heat flow characteristics. Results of the measurements performed thus far are depicted and they demonstrate an adequate performance of the measurement system in terms of both validity and reliability, suggesting that this instrument can present a solid base for studying and testing thermal storage materials.

Farther experiments are proposed to focus upon identifying additional chemically and thermally stable PCM/HTF combinations for thermal storage as well as further advancement of the system aimed at running long-term multicycle tests for PCM samples.

Keywords: Phase change materials, Latent heat storage, Heat transfer performance, Thermal storage measurements and analysis.

Nomenclature:

CSP – concentrating solar power

DSC – differential scanning calorimetry

DTA – differential thermal analysis

ΔH_{HTF} – change in enthalpy of the HTF

ΔH_{loss} – thermal losses from the system

ΔH_{PCM} – change in enthalpy of the PCM

$\Delta Hsys$ – change in Enthalpy of the system

ΔH_{Vessel} – change in enthalpy of vessel material

HTF – heat transfer fluid

L(R)HS – left(right) hand side

m_{HTF} - mass flow rate (g/s) of HTF

PCM – phase change material

RHTS - reflux heat transfer storage

TGA - thermo-gravimetric analysis

T_{HTF} – temperature of HTF

$T_{Furnace}$ – temperature of furnace

T_{PCM} – temperature of PCM

1. Introduction

Phase change materials (PCM) considered in the literature for latent heat storage integrated into CSP systems for electricity generation are mainly inorganic salts (pure substances and eutectic mixtures), e.g. $NaNO_2$, $NaNO_3$, KNO_3 etc., operational in the temperature range from about 250 to 550°C. PCMs designated for thermal storage are usually composed of technical grade materials rather than pure chemicals for which accurately measured thermochemical data are tabulated in literature. For the development of an efficient thermal storage system it is crucially important to carry out calorimetric measurements and lifetime tests working with representative materials samples under heating/cooling conditions closely approaching the highly transient thermal storage process of a full scale system.

The calorimetric technique widely applicable for the measurement of the enthalpy of solid and liquid substances used for thermal storage, such as various inorganic salts, metal alloys, etc., is based on the DSC/DTA method [1, 2]. However, a single method cannot be suitable for all possible materials and, moreover, it is always useful to have thermochemical data obtained from different methods to allow more accurate and statistically reliable results. Specifically, for latent heat storage employing phase change materials, it is very important to run the thermal storage cycles of charging and discharging inside a calorimetric system in order to measure temperatures along with the evolved heat directly. In the literature different types of custom-built high-temperature calorimeters are discussed [3]. However, each of such devices was designed to solve a specific problem and cannot be readily adopted to accommodate the thermal storage testing conditions.

A lab scale apparatus capable for testing thermal storage materials simultaneously with carrying out calorimetric measurements and studying heat transfer effects developed in the system was reported elsewhere [4]. This system was initially designed for investigating the compatibility and thermal stability of storage materials used in the RHTS (reflux heat thermal storage) system developed as part of the EU-funded FW6 DISTOR project. It demonstrated highly efficient heat transfer characteristics and the capability to operate as a calorimeter aimed to quantify the latent heat storage variability during thermal charge and discharge cycles.

This apparatus consists of a temperature controlled furnace for heating a sampler vessel containing PCM (max 1.5 kg) to a temperature over the melting point (up to 400^{o}C). Along with PCM, the sampler vessel contains some amount of HTF (heat transfer fluid, e.g. thermal oil Dowtherm-A, about 200-300 ml), which is boiling inside the vessel and its vapor is used to transfer heat from the PCM sample to a water filled condenser, both connected in a closed loop by pipes and a coiled heat exchanger. A number of thermocouples were set in the PCM, HTF, and water bulk to monitor the temperatures continuously. Multiple cycles with different rates of heat charge and discharge were made possible by controlling the furnace temperature ramp and the HTF vapor flow rate. The heat flow in the system could be evaluated in accordance with the heat balance, so that the amount of energy supplied to the water is equal to the decrease of enthalpy of the sampler vessel, taking into account the calibrated heat losses.

In response to the Task 4 of Work Package 15 “New Measurement System for PCM storage” including the objectives of “Development of a measurement concept for calorimetric and heat flow parameters under the saturated pool boiling conditions of high-temperature heat transfer fluids, in lab scale (WEIZMANN)” and “Design and construction of a prototype measurement device (DLR, WEIZMANN) we decided to adopt the RHTS concept for calorimetric measurements and testing PCM for latent heat energy storage systems. This involved making modifications to the existing lab scale apparatus necessary to promote the following functions of the measurement system under development:

- Accurate heating control, monitoring and recording of temperature and pressure in numerous points in the system using a data acquisition system;
- Accurate and reliable regulating of heat discharge using a metering valve in the HTF vapor flow loop;
- Minimal thermal losses to the environment;
- Working with different PCM samples including molten salts and metal alloys;
- Developing a modeling program to analyze the obtained data and evaluate the essential thermal storage parameters.

2. Background of the RHTS concept

The RHTS concept is based on a synergistic effect of phase change processes of melting and vaporization occurring in the thermal energy storage medium. For this purpose, a low melting point HTF, for instance liquid metal or synthetic organic oil, is added to the PCM, to deliver thermal energy between the storage medium and a heat sink (e.g. a heat exchanger, steam generator) located out of PCM via evaporation and reflux condensation of the HTF. This heat transfer pattern is similar to one effectively utilized in thermosyphons, heat pipes and pool-boilers. It is important that the storage vessel be thoroughly evacuated of water vapors and other gases in the beginning and kept continually leak-tight for both vacuum and pressure conditions.

Choosing the HTF involves several prerequisites including high-temperature stability, chemical compatibility and mutual insolubility with the PCM, non-corrosiveness to the structural materials, low density in comparison with the PCM, and a sufficient vapor pressure (about 1 bar abs) at the operating temperature.

Feasibility of this storage concept was successfully demonstrated using PCM-HTF systems composed respectively of sodium chloride salt and sodium metal for a storage temperature of 800^{o}C [5] and zinc metal alloy (Zn70Sn30) and thermal oil Dowtherm-A for 370^{o}C [4].

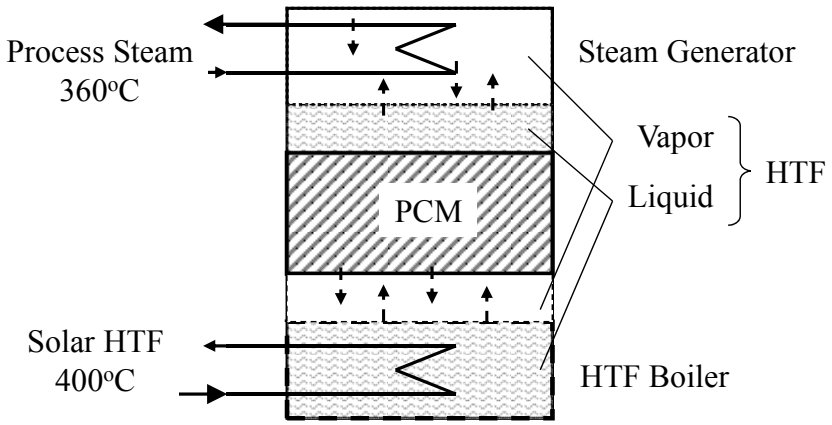

Figure 1. Schematic diagram of the RHTS concept. In the case of the same HTF used in the solar field and in the storage, the bottom heat exchanger is no longer needed.

Figure 1 illustrates the RHTS concept intended to produce high temperature steam for a parabolic through CSP plant when the solar steam generation process is temporarily interrupted. HTF is used to transfer heat between the thermal storage medium - PCM and two heat exchangers (HE) placed externally to the PCM compartment at the bottom and the top of the storage vessel. The top HE, i.e. steam generator, is fed with high pressure water (return condensate) to produce superheated steam during the storage discharge cycle. The bottom HE is used to charge the thermal storage. It is immersed in the liquid HTF and connected to the solar working fluid, e.g. a flow of solar superheated steam or solar-heated synthetic oil. During heat charge cycles, due to pool-boiling of the HTF, there is intensive flow of vapors up through the transport channels distributed in the PCM. By condensation directly on the surface of the PCM, the latent energy of vapors is transferred across the PCM bulk. On discharge, the heat flow direction is reversed. The hot PCM causes the liquid HTF to evaporate and the vapors transmit heat to the top located steam generator via the mechanism of condensation.

3. Methodology of testing PCM

The testing procedures for thermal storage materials regarding the target temperature of 400^{o}C are described below on the example of a PCM-HTF system examined in the initial stage of the RHTS development [4]:

- **PCM**: Zinc-Tin alloy containing 70%wt Zn (Zn70Sn30). This substance is a non-eutectic (hypoeutectic) composition that melts gradually between the eutectic -198.5^{o}C and liquidus - 370^{o}C temperatures. It needs a high-temperature HTF close to 400^{o}C, such as exiting a solar parabolic troughs system, to charge the storage. On discharge, the release of heat is due mainly to the latent heat of zinc solidification and partly to the sensible heat of the dual-phase (liquid-solid) mixture of the alloy.
- **HTF**: eutectic mixture of 26.5% biphenyl and 73.5% diphenyl oxide which is produced commercially as a high-temperature (max 400^{o}C) thermal oil (e.g. Dowtherm-A, Therminol VP-1). Equilibrium vapor pressure of this HTF is about 7.2 bars at the storage temperature of 370^{o}C.

Specimens of the chosen PCM and HTF chemicals were subjected, separately and jointly, to a sequence of laboratory testing procedures under a constant temperature of 400^{o}C and maintaining a variable temperature between 200 and 400^{o}C. Alloy Zn70Sn30 was specifically manufactured using the base metals of technical-purity grade by Numinor Chemical Industries Ltd (Israel). The major impurity determined in the product was iron which was the material of the crucible employed in the alloy production. The HTF was purchased as a commercial product Dowtherm-A produced by Dow Chemical Co.

3.1. Ampoule tests

The test procedure included the following steps:

- Preparing hermetically sealed glass ampoules (10 ml capacity) filled with a few grams of Zn70Sn30 alloy (particles of a size 2-3mm) along with a few milliliters of the liquid HTF. In some of the ampoules, stainless steel (316L) pieces were added to test the effect of a potential storage structure material.
- Placing the ampoules into a laboratory high-temperature oven and holding them at 400^{o}C at least 8 hours. The heating routine was repeated 3-4 times at regular intervals with each ampoule.
- Post-test visual inspection of the ampoules at ambient temperature for: integrity (some might burst), change of color, physical state, additional phases, etc.
- Examining the content of ampoules by means of Differential Thermal Analysis (TA Instruments TG/DTA Q600 system) and FTIR Spectroscopy (Brukner FTIR Analyzer TENSOR 27).

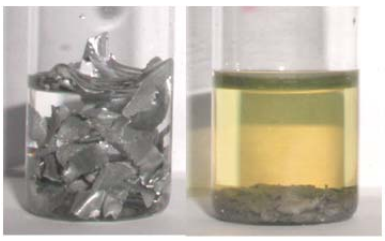

Figure 3. A glass ampoule before (left) and after (right) heating at 400^{o}C for 8 hours. The ampoule was initially loaded with Zn70Sn30 particles and Dowtherm-A, the colorless liquid, and sealed by welding.

As is shown in Fig. 3, some visible changes could be typically observed after the first heating of the test ampoules:

1. The solid particles became fully fused as a result of heating above the liquidus point, 370^{o}C;
2. The liquid, first transparent and colorless, appeared to be yellowish-red. The same change in color occurred when the HTF was sealed in ampoules and heated above 200^{o}C with no presence of supplemental materials. This change of color (no difference in the FTIR spectrum could be detected) has no consequences on the performance of the thermal storage;
3. No further visible modifications of the ampoules content were discovered after repeating the heating procedure several times.

About 20 ampoules containing PCM-HTF-Steel samples were tested accordingly. All of them, without exception, showed satisfactory results in terms of thermal stability and compatibility of the storage materials verified by DTA and FTIR analyses. In addition, the remarkable thermal stability of the tested PCM-HTF system was verified under continuous 30-days heating in the glass ampoules at 400^{o}C.

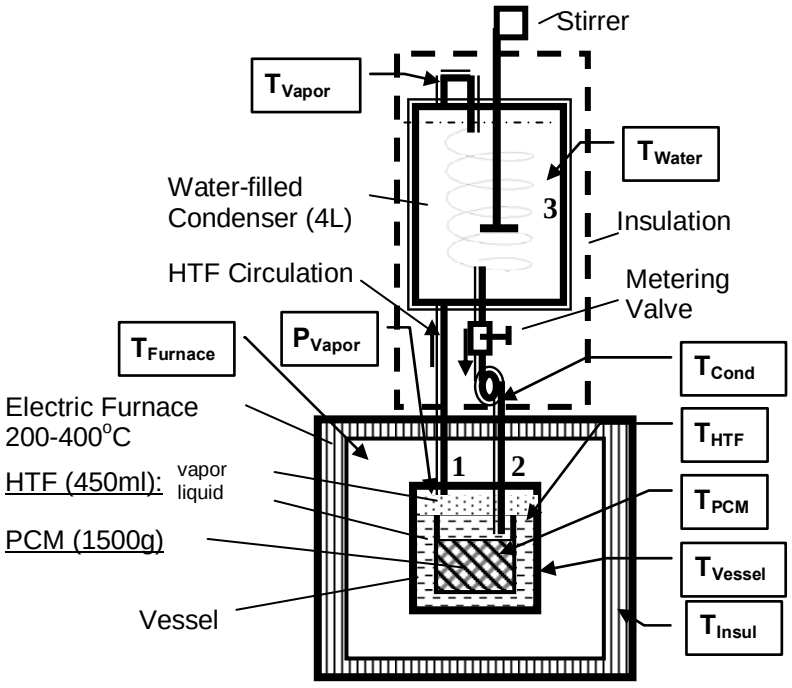

Figure 4. The lab set-up design composed of the sampler vessel containing PCM and condensed HTF, electric furnace, metering valve and water-filled condenser. Points of measurements are shown indicating: T-temperature, P-pressure.

Figure 4 represents a diagram of the laboratory set-up used for testing the storage materials under thermal conditions typical of a full-scale system. A temperature controlled furnace is used to heat the sampler vessel containing alloy Zn70Sn30 (1500 g) and Dowtherm-A (450 ml) to a temperature of 390-400°C. As shown in the diagram, the sampler vessel together with vertical tubes (1) and (2) and coil (3) form a closed loop for HTF flow. A metering valve (Swagelok – BMRW, V51), installed on the tube (2) is used to block the fluid flow while heating of the sample is activated. The valve has a micrometric regulator so that flow can be metered very accurately, over a range of 0 to 6 turns, which corresponds to a flow of 0 to 1 mL/min (based on water calibration) in the range of HTF pressure utilized in the system, 0 – 10 bar.

Table 1. Points of measurements applied in the heat cycling tests as shown in Fig. 4.

Parameter and Maximal Experimental Value	**Notation**	**No. of Points**	**Sensor**	**Accuracy**
PCM temperature inside the sampler vessel, 380^{o}C	T_{PCM}	2	TC type K	1.5^{o}C
HTF temperature inside the sampler vessel, 400^{o}C	T_{HTF}	2		
HTF vapor temperature in tube (1), 400^{o}C	T_{Vapor}	1		
HTF condensate temperature in tube (2) , 80^{o}C	T_{Cond}	1		
Furnace temperature, 450^{o}C	$T_{Furnace}$	3		
Water bulk temperature, 60^{o}C	T_{Water}	6	TC type T	0.5^{o}C
HTF vapor pressure in the sampler vessel, 10 bar	P_{Vapor}	1	Pressure transducer	0.05 bar

After melting the PCM sample and reaching the required temperature, the furnace is switched off and the valve is opened to allow HTF to flow and circulate. During that period the heat of the storage is transferred to the water condenser by HTF due to the subsequent processes of liquid evaporation taking place in the sampler vessel, rising of the vapors in the tube (1) and vapor condensation occurring in the coil. By gravity the HTF condensate returns through the tube (2) back to the sampler vessel. The points of measurements include temperature in different location of the system and HTF vapor pressure, as shown in Figure 4 and specified in Table 1. The experimental data are transferred to a PC using a data acquisition system.

Multiple cycles with different rates of heat charge and discharge were made possible by controlling the furnace and metering valve correspondingly. After each cycle the hot water was replaced with the same quantity of the room temperature water. According to the energy balance, the heat supplied to the water equates the decrease of enthalpy of the sample taking into account the heat losses evaluated in specifically performed experiments beforehand.

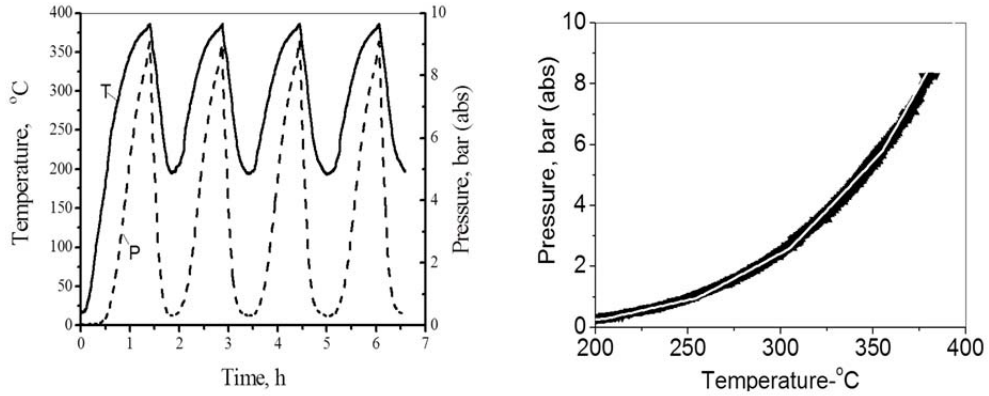

Figure 5. Typical PCM temperature (T) and HTF vapor pressure (P) experimental data measured inside the sampler vessel of the lab set-up. LHS: a fragment of the multicycle test; RHS: vapor pressure P vs. temperature T (white curve – equilibrium data for Dowtherm-A [6], black strip – experimental points obtained from one thermal cycle of sample heating and cooling).

In the case of proper operation, the vapour pressure of HTF should follow closely the thermodynamic equilibrium data available for this fluid. If the thermal fluid fails due to thermal decomposition or reacting with PCM or other materials in direct contact, a significant deviation of pressure from the equilibrium value at the operating temperature could be expected. In total, more than a hundred thermal cycles such as shown in Fig. 5-LHS, with the same load of storage materials were performed. Similar to the run depicted in Fig. 5-RHS, all the other experimental results exhibited without exception excellent thermal stability of the Zn70Sn30 - Dowtherm-A storage materials system under the corresponding variations of temperature between 200 and 380^{o}C.

4. Adjustment of the measurement system

Some necessary modifications to the lab system were made to allow more accurate measurements and evaluation of the calorimetric and heat transfer properties of PCM samples.

4.1. Estimation and Control of Heat Losses

It is important to minimize thermal interaction between the sampler vessel and the furnace on the stage of discharge, when the furnace is off and the heat is released from the storage to the water condenser. Depending on the temperature difference δT between the furnace interior and the PCM inside the vessel, the heat transfer between the two bodies has a direction either toward (when δT>0) or opposite (when δT<0) the vessel. Quantitatively, the furnace's effect upon the thermal storage value could be quite significant and therefore should be dealt with accordingly.

An estimation of the heat flow to/from the vessel was approached by discharging the system at a specific flow rate and varying several furnace parameters, such as the angle of the furnace door opening and the operation of the furnace convection fan. These factors revealed a strong influence on the heat balance in the system thus have proven themself as effective means of thermal isolation (the method used to reduce heat transfer) for the sampler vessel. A series of experiments was conducted to identify the extent of furnace door opening that was necessary to maintain thermal equilibrium between the vessel and the furnace ($\delta T = T_{Furnace} - T_{PCM} \sim 0$, referring to points of measurement shown in Fig. 4). This allowed comparing the system heat balance with and without vessel 'isolation' in order to estimate the thermal effect of the furnace during the storage heat discharge.

Parameters for heat discharge in both the isolated and non-isolated tests were determined for the max HTF mass-flow rate (full opening of the valve) by quantifying the amount of heat transferred from the storage vessel to the water-filled condenser using the equations (1) – (3) below:

$$\Delta H_{loss} = \Delta H_{sys} - \Delta H_{H_2O} \tag{1}$$

Here, ΔH_{loss} is the thermal losses from the sampler vessel, calculated from the difference between ΔH_{sys}, the total change in enthalpy of the storage system (defined below), and ΔH_{H_2O} the enthalpy change of the water contained in the water condenser.

$$\Delta H_{sys} = \Delta H_{PCM} + \Delta H_{HTF} + \Delta H_{Vessel} \tag{2}$$

Here, ΔH_{sys} is the sum of the change in enthalpy of all components of the system: the PCM, the HTF and the stainless steel vessel.

$$\Delta H_{H_2O} = m_{H_2O} \quad C_p \quad \Delta T_{H_2O} \tag{3}$$

Here, ΔH_{H_2O} is the change in enthalpy of the water mass m_{H2O} contained in the condenser, calculated from C_p, the specific heat of water (4.1806 J/g K) and the change in temperature of the water over the course of the experiment.

The temperature measurements are shown in Fig. 6, and the furnace parameters and heat balance results are outlined in Table 2.

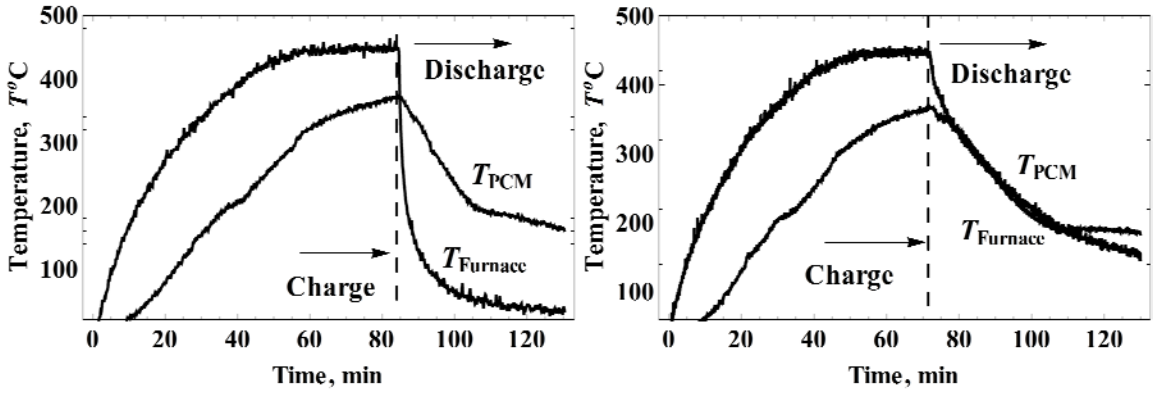

Figure 6. Graphs showing the charge-discharge cycles under the system conditions of non-'isolation' (a) and 'isolation' (b). Both discharge tests were conducted under full HTF flow and other conditions as outlined in Table 2. The isolated case shows the temperature equilibrium attained by the furnace fan operation and furnace door partial closure. The dashed line indicates the end of charge and beginning of discharge.

Table 2. System parameters for non- and 'isolated' storage discharge. The isolation column indicates whether (Y) or not (N) furnace parameters were adjusted to control thermal insulation of the vessel used. Furnace Fan and Door Angle show the internal convection fan state and extent of door opening utilized upon discharge (an angle of 0 indicates a fully closed and 90^{o} – the fully opened state). The losses column refers to the results of the heat balance between the ΔH_{SYS} and ΔH_{H20}. All values of ΔH are in kJ. Measurements are based upon a 300 sec period of discharge.

Isolation	Furnace Fan	Door Angle	ΔH_{SYS}	ΔH_{PCM}	ΔH_{HTF}	ΔH_{Ves}	ΔH_{H20}	Losses
N	Off	90°	150	41	33	76	91	59
Y	On	5°	127	31	31	64	132	-5

Figure 6(b) shows that by adjusting the system parameters upon discharge as outlined in Table 2, the proper isolation of the storage vessel is achievable, leading to the temperature equality $T_{Furnace} \approx T_{PCM}$. Upon non-isolated discharge of the system 59 kJ was lost from the system, while under isolated conditions a relatively small negative value of -5 kJ was calculated. It is expected that this value falls within the signal to noise ratio of the temperature measurements and subsequent calorimetric calculations, and can essentially be regarded as almost zero. In principle, a higher resolution of thermal losses is possible, if necessary, by a finer tuning of the system parameters.

4.2. HTF Flow Rate Determination

The natural convection circulation flow of HTF through the system was calculated from temperature measurements and enthalpy calculations for the HTF, PCM and water filled into the condenser. This value is important as it is the principal parameter used in heat balance calculations and directly governs the quantity of heat released from the storage. Several influential variables of the process were constrained by keeping the temperature of the sampler vessel constant over the course of discharge to obtain a constant flow and to reduce error which could have been introduced to the calculation from changes in HTF pressure, should the system be discharged as per the normal operating procedure. This was achieved by optimising furnace parameters of the system, and maintaining a constant PCM/HTF temperature over the course of the experiments, as shown in Fig. 7.

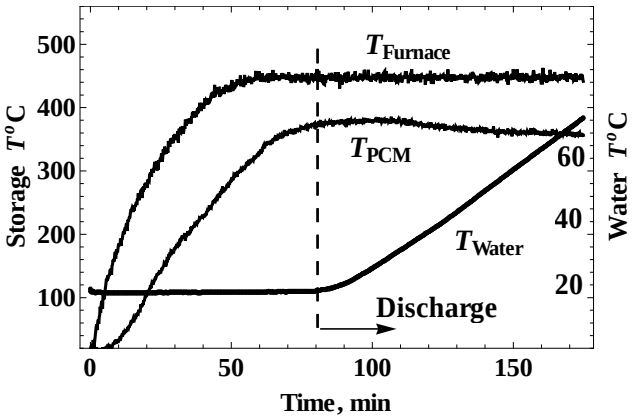

Figure 7. Temperature profile of constant vessel heating for the determination of HTF flow rate. This experiment was carried out using a constant furnace temperature of 450 °C, 40% opening of the valve. The furnace door was completely closed and the fan was in operation. $T_{Furnace}$ refers to the temperature of the furnace and T_{PCM} is the temperature of the Zn70Sn30 alloy and T_{Water} is the water temperature. The linearity of the water graph results from a constant flow rate of the HTF under the conditions of the experiment.

System parameters were optimized for two flow rates, 40% and 60% of the maximum flow achievable by the system. Flow rate was determined by calculation using the following equation:

$$Q_W = \Delta Q_{HTF} = \dot{m}_{HTF} \bullet \Delta H_{HTF} \bullet \Delta\tau \tag{4}$$

Where, Q_w is the amount of heat supplied to the water in the water-filled condenser, ΔQ_{HTF} represents the change in HTF heat, $\dot{m}_{HTF}$ is the mass transfer rate (g/s) of the HTF through the system, ΔH_{HTF} is the change in enthalpy of the HTF over the temporal period defined by $\Delta\tau$. Equation 4 was rearranged to solve for the mass transfer rate of HTF ($\dot{m}_{HTF}$) by:

$$\dot{m}_{HTF} = \frac{Q_w}{\Delta H_{HTF} \bullet \Delta\tau} \tag{5}$$

An average per % flow rate was calculated as about 8.10^{-3} g/s/%_valve_opening, based on several experiments conducted.

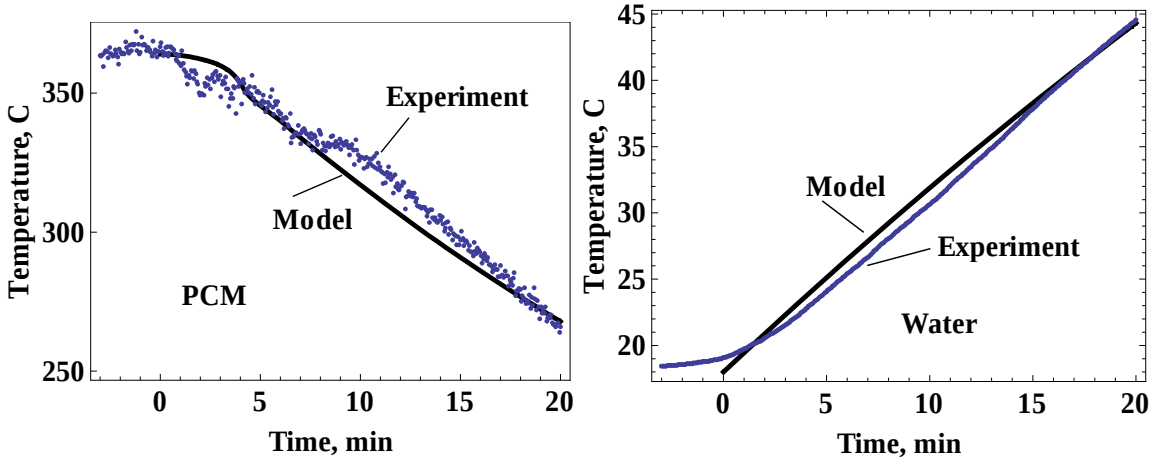

Figure 8. Comparison of the simultaneous temperature measurements for PCM (Zn70Sn30) and water during a heat discharge cycle with model simulation results.

4.3. Thermal Analysis Model

In total, there were more than a hundred thermal cycles performed with different loads of storage materials. The obtained experimental data were used in the development and validation of a thermal analysis model based on heat balance equations written for the transient RHTS process activated in the measurement system:

$$\delta q_1 = m_{PCM} \frac{d\Delta H_{PCM}[T_{PCM}[t]]}{dt} \tag{6}$$

$$\delta q_2 = M_{HTF} \frac{d\Delta H_{HTF}[T_{HTF}[t]]}{dt} \tag{7}$$

$$\delta q_3 = m_{HTF}(\Delta H_{HTF}\ [T_{HTF}[t]] - \Delta H_{HTF}[T_C[t]] \tag{8}$$

$$\sum_3 \delta q_i = Q_{loss} \tag{9}$$

$$m_{H_2O} c_p \delta T_{H_2O}[t] = \delta q_3 - q_{loss} \tag{10}$$

$$k\, A\, \Delta T[t] = \delta q_1 \tag{11}$$

In the set of expressions above, Eq. (6) describes the change of PCM enthalpy ΔH_{PCM} (alloy quantity m_{PCM}, bulk temperature T_{PCM}) in time t, Eq. (7) - enthalpy change of liquid HTF held in the sampler vessel (fluid quantity M_{HTF}, bulk temperature T_{HTF}), Eq. (8) – the heat transferred by vapor flow (HTF circulation mass rate m_{HTF}, condensate temperature T_C)

between the sampler vessel and the water container, Eq. 9 is a heat balance equation for the sampler vessel and transport tubes, including heat losses Q_{loss} (convection and radiation), Eq. 10 is a heat balance equation for the water container (water quantity m_{H2O}, specific heat c_p, bulk temperature T_{H2O}), including heat losses q_{loss}, and Eq. 11 determines the heat transfer coefficient k at the PCM-HTF interface in the sampler vessel, taking into account the surface area A and mean temperature difference between the substances ΔT.

The adequateness of the thermal analysis model to experimental data is shown in Fig. 8. The model solutions were obtained using the numerical package of Mathematica 8. Enthalpies and other properties of the storage materials needed in calculations were measured in the lab, specifically for the Zn-based alloy PCM using the TGA instrument, and regarding Dowtherm-A and stainless steel the data were taken from the literature.

5. Molten salt Demonstration Test and Evaluation

The choice of PCM involves a number of options taking into consideration the factors of high-temperature durability, chemical compatibility with the HTF, the desire for a high latent heat value and density of the substance, commercial availability and the price. Along with the metal alloy investigated previously, we intend to examine some cheap and widely available thermal storage materials that can be utilized for latent heat storage based on the RHTS technology.

For this purpose, PCM and HTF systems based on nitrate salts of Na/KNO_3 and Dowtherm-A have been set for lab experiments using the developed methodology for testing thermal storage materials (section 3). This included high-temperature test-tube examination and calorimetric measurements using the calorimetric set-up developed.

The measurements conducted for potassium nitrate salt KNO3, melting point 334^{o}C, are depicted below showing the main results of thermal analysis and heat flow evaluation performed.

5.1. Testing procedures

Figure 9 presents enthalpies of the selected storage materials system based on the literature sources that were verified by lab measurements with the particular chemical samples in use.

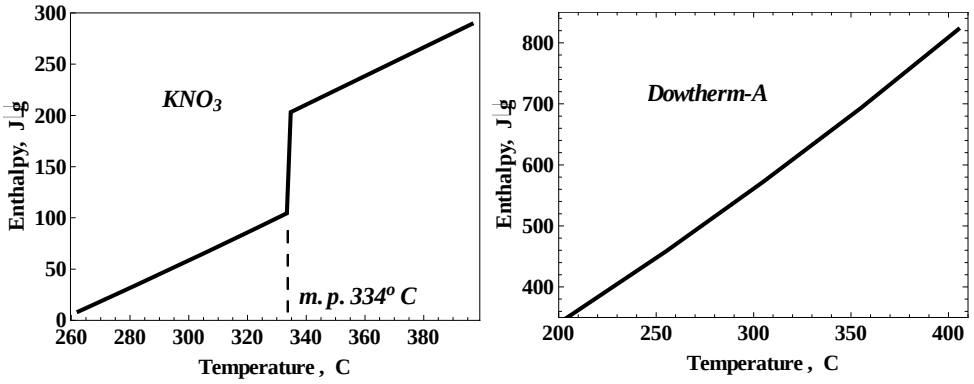

Figure 9. Enthalpy data for KNO_3 [7] and Dowtherm-A (liq) [6] used in the thermal analysis.

The combination of KNO_3 and Dowtherm-A was tested in glass ampoules by raising the oven temperature above the salt melting point of 334°C, up to 360°C, for a various time periods extending to a few tens hours, Fig. 10 (LHS). The results of post-test analyses done using the TGA/DTA and FTIR instruments were favorable in terms of the adequate chemical stability and compatibility of the selected storage materials, verified concerning the PCM melting point and the HTF IR spectrum and vapour pressure vs. temperature.

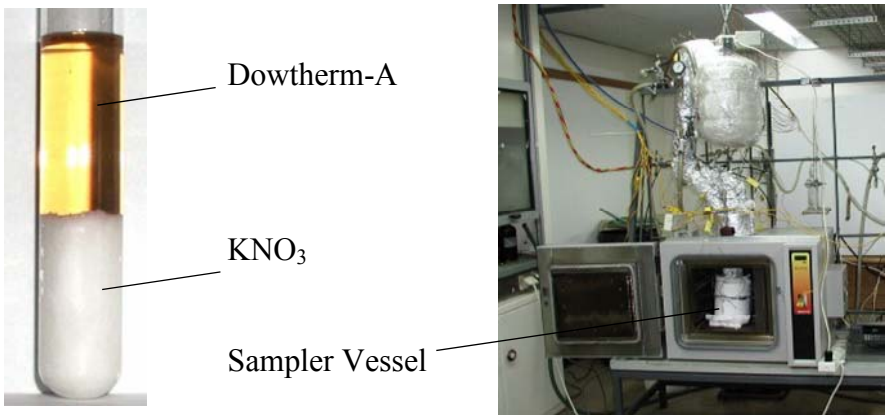

Figure 10. The LHS photo shows a glass ampoule containing a few grams of potassium nitrate and Dowtherm-A after heating during several hours at a temperature 360°C. In the RHS photo is the measurement system with the sampler vessel located in the furnace.

About 800 g of KNO_3 and 250 ml of Dowtherm-A were charged into the sampler vessel, which was set up in the furnace, as shown in Fig. 10 (RHS). The calorimetric system was run under various HTF mass flow rates maintaining the conditions of optimal

"isolation" and upper charge temperature of 360°C. More than ten different cycles were performed successfully without showing symptoms of abnormal operation.

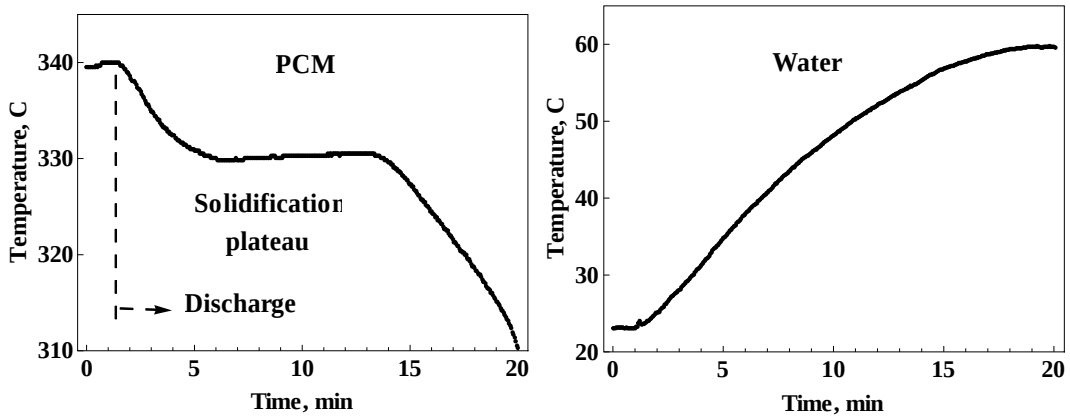

Figure 11. The simultaneous temperature profiles measured in the molten potassium nitrate salt - T_{PCM} and water - T_{Water} under the full HTF mass flow, 0.8 g/s. The locations of thermocouples are as shown in Fig. 4.

5.2. Experimental results

The molten salt temperature profile (Fig. 11, LHS) explicitly shows the constant temperature solidification process characteristic for crystalline substances, as it is the potassium nitrate salt subjected to the described measurements.

The results of thermal analysis calculations revealed the following values of calorimetric and heat transfer parameters of the KNO_3 – Dowtherm-A system for the heat discharge process demonstrated:

- PCM thermal storage capacity: 100 j/g,
- HTF circulation rate m_{HTF}: 0.8 g/s,
- PCM-HTF bulk temperature difference ΔT: < 10 K,
- PCM-HTF interface:
    - heat flux: ~ 10 kW/m^2,
    - heat transfer coefficient k: ~ 1 kW/m^{2}K.

The obtained estimates indicate very high heat transfer rates resulting from such factors as nucleate boiling of HTF in the sampler vessel, intensive vapor generation and natural circulation of the fluid within the closed loop. The overall thermal conductivity of the calorimetric system could be represented as,

$$\lambda \approx \frac{\delta q_1 \, A}{\delta T \, h} \tag{12}$$

Here, δT is a temperature difference between the sampler vessel and the entrance to the water container (~ 1-2 K), h is a length of the transport tube 1 (Fig. 4, 1.2 m). The estimated value of λ~500 W/m-K is comparable to the thermal conductivity of copper metal (401W/m-K). Based on this result, the performance of the calorimetric set-up can be compared to the performance of the other super-efficient thermal systems utilizing reflux condensation heat transfer, such as thermosyphons and pool boilers [8].

6. Conclusion

The development and design of a lab PCM measurement system for calorimetric and heat flow parameters of thermal storage have recently been accomplished and its performance has been demonstrated by testing two different PCM samples: Zn-based alloy, Zn70Sn30, and potassium nitrate salt, KNO_3. In the present configuration the apparatus provides thermal measurements for PCM samples of about 800-1500g in the temperature range between 200 and 400^{o}C (the upper limit temperature of the HTF used) and enables simultaneous studying calorimetric properties of the loaded PCM and heat transfer effects developed in the system.

The measurement system is accompanied with a mathematical model based on heat balance equations written for the transient heat transfer process activated in the calorimetric set-up that was developed to assist in performing the thermal analysis including the evaluation of calorimetric and heat transfer properties of PCM under test.

Over the next year, work is planned to focus upon identifying and testing chemically compatible and thermally stable PCM/HTF combinations having a melting/eutectic temperature close to 400^{o}C, as well as the further modification of the measurement system aimed at long-term multicycle tests of the PCM samples by upgrading the data acquisition software and incorporating a simpler structure for the sampler vessel.

5. References

[1] Zalba B, Marin JM, Cabeza LF, Mehling H. Review on thermal energy storage with phase change: materials, heat transfer analysis and applications. App Thermal Eng 2003; 23: 251–283.

[2] Kenisarin MM. High-temperature phase change materials for thermal energy storage. Renew Sustain Energy Rev 2010; 14: 955-970.

[3] Dincer I, Rosen M. Thermal energy storage: systems and applications. John Wiley and Sons, 2010.

[4] Adinberg R, Zvegilsky D, Epstein M. Heat transfer efficient thermal energy storage for steam generation. Energy Convers Manag 2010; 51: 9-15.

[5] Adinberg R, Yogev A, Kaftori D. High temperature thermal energy storage. J Phys IV France 1999; 9: 89–94.

[6] Dowtherm A Technical Data Sheet. http://www.dow.com/heattrans/tech/data.htm [accessed Sept. 2011].

[7] HCS Chemistry 5.0 Outokumpu Research Oy, Pori, Finland.

[8] Collier JG and Thome SR. Convective boiling and condensation. Clarendon Press, Oxford, 3rd edition 2001.